RECENT PROGRESS IN GENERAL RELATIVITY

PETER HINTZ AND GUSTAV HOLZEGEL

ABSTRACT

We review recent progress in general relativity. After a brief introduction to some of the key analytical and geometric features of the Einstein equations, we focus on two main developments: the stability of black hole solutions, and the formation, structure, and dynamical stability of singularities.

MATHEMATICS SUBJECT CLASSIFICATION 2020

Primary 83C05; Secondary 83C57, 35L05, 35B40, 35L81

KEYWORDS

Einstein's field equations, black hole stability, Strong Cosmic Censorship

INTERNATIONAL CONGRESS OF MATHEMATICIANS 2022 JULY 6–14

Proc. Int. Cong. Math. 2022, Vol. 5, pp. 3924–3984
DOI 10.4171/ICM2022/128

Published by EMS Press

1. INTRODUCTION

The objective of this article is to describe recent progress in the mathematical analysis of the Einstein equations of general relativity. General relativity is the theory of gravitation postulated by Einstein in 1915. It superseded the Newtonian theory and rose to one of the best experimentally tested physical theories we have. The Einstein equations can accurately describe violent astrophysical processes happening in our universe (such as the merger of black holes), they provide a model for the evolution and dynamics of our entire universe in cosmology, and they are also central for the functioning of the ubiquitously used GPS system on Earth. Recent experimental breakthroughs such as the detection of gravitational waves, a prediction of Einstein's theory, have inspired new developments in mathematics and physics some of which we shall discuss below.

This article consists of three main parts, which are aimed at readers with potentially different levels of expertise. The first part (Section 1) contains an introduction to some of the basic geometric and analytic principles governing the study of general relativity (with emphasis on the issue of diffeomorphism invariance of the governing equations). It also includes examples of black hole solutions and a discussion of their geometry. This part is intended for mathematicians who are perhaps familiar with the theory of partial differential equations but have otherwise little prior knowledge of general relativity.

The second and main part (Section 2) contains a review of recent mathematical results that have been obtained in the study of the stability of black holes. This part is aimed mostly at readers who have had some previous experience with the study of wave equations on curved backgrounds; familiarity with the Einstein equations will be useful for the results on nonlinear or linearized gravity. Research during the past 15–20 years pioneered the techniques that led in particular to the powerful nonlinear results which have been obtained in the past five years and that we shall describe in more detail. We have kept the discussion rather informal: theorems are often stated rather loosely in order to avoid introducing too much notation; additional details are provided in the text. We hope that our descriptions of the main ideas of the proofs can serve as an invitation to delve into the papers in this area in some more detail.

The third part (Section 3) is concerned with the issue of singularities. We shall discuss the structure of singularities appearing inside black holes as well as their stability, which is related to Penrose's famous *Strong Cosmic Censorship* conjecture. We also discuss results concerning *naked singularities*, which are related to *Weak Cosmic Censorship*.

Unfortunately, in this overview we cannot do justice to the wide range of developments in mathematical relativity. The choice of topics is influenced both by our personal expertise and taste. In particular, we almost exclusively focus on the vacuum equations. There are many exciting developments that we will not be able to discuss: these include recent progress on the weak limit of the Einstein equations (e.g., Burnett's conjecture [32, 123], also [155]) and the structure and dynamics of cosmological singularities (stable big bang formation [82, 83, 181]), among others.

1.1. The Einstein equations

From a mathematical point of view, the Einstein equations constitute a set of nonlinear partial differential equations formulated in the language of differential geometry with the dynamical variable being a Lorentzian manifold $(\mathcal{M}, g)$:

$$\mathrm{Ric}(g) - \frac{1}{2}Rg + \Lambda g = 8\pi\mathbb{T}. \tag{1.1}$$

Here $\mathrm{Ric}(g)$ and $R = \mathrm{tr}_g \mathrm{Ric}$ denote the Ricci tensor and scalar curvature of $(\mathcal{M}, g)$, Λ is the cosmological constant, and $\mathbb{T}$ is the stress–energy–momentum tensor of the matter present in the spacetime. Below we shall mostly restrict attention to the vacuum case $\mathbb{T} = 0$ for which the equations (1.1), unlike their Newtonian analogue, already exhibit extremely rich dynamics, although comments will be made about the analysis of spacetimes with matter. Furthermore, we will focus on the physical case $\dim \mathcal{M} = 4$.

Applying the trace reversal operator $\mathsf{G}_g : T \mapsto T - \frac{1}{2}g\,\mathrm{tr}_g T$ to equation (1.1) yields the following equivalent form of the Einstein equations:

$$\mathrm{Ric}(g) - \Lambda g = 8\pi\left(\mathbb{T} - \frac{1}{2}g\,\mathrm{tr}_g\,\mathbb{T}\right) \quad (= 0 \text{ in vacuum}). \tag{1.2}$$

1.2. The Cauchy problem and generalised harmonic gauges

While not immediate from the coordinate independent formulation (1.1), from a PDE point of view (1.1) should be viewed as a hyperbolic system of equations, i.e., as a system admitting an appropriate initial value problem. The geometric notion of initial data is as follows:

Definition 1. A triple $(\Sigma, \bar{g}, K)$ consisting of a smooth Riemannian manifold $(\Sigma, \bar{g})$ and a smooth symmetric 2-tensor K on Σ is called a (smooth) vacuum initial data set for (1.1) (i.e., with $\mathbb{T} = 0$) if it satisfies the constraint equations

$$\bar{R} + (\overline{\mathrm{tr}}\,K)^2 - |K|^2_{\bar{g}} = 2\Lambda, \quad \overline{\mathrm{div}}\,K - \mathrm{d}\,\overline{\mathrm{tr}}\,K = 0. \tag{1.3}$$

Theorem 1 ([39, 40, 180, 187]). *Let $(\Sigma, \bar{g}, K)$ be a smooth vacuum initial data set. Then there exists a unique smooth maximum Cauchy development, i.e., an $(\mathcal{M}, g)$ with the property that*

(1) $(\mathcal{M}, g)$ *solves* (1.1) *with* $\mathbb{T} = 0$.

(2) *There exists an embedding $i : \Sigma \to \mathcal{M}$ such that $i(\Sigma)$ is a Cauchy hypersurface in $(\mathcal{M}, g)$ and such that the induced metric and second fundamental form of the embedding agree with $\bar{g}$ and K.*

(3) *If $(\tilde{\mathcal{M}}, \tilde{g})$ also satisfies* (1) *and* (2)*, then there exists an isometric embedding $(\tilde{\mathcal{M}}, \tilde{g}) \to (\mathcal{M}, g)$ commuting with the embeddings of Σ.*

We remark that the constraint equations (1.3) are the Gauss and Gauss–Codazzi equations induced by (1.1) on Σ and thus necessary conditions. We also note that for simplicity we have stated the theorem in the smooth category although one typically proves Sobolev versions of the result. Finally, the manifold $\mathcal{M}$ is diffeomorphic to $\mathbb{R} \times \Sigma$ [21].

Theorem 1 allows one to talk sensibly about the dynamics of solutions to the Einstein equations. This will allow us to formulate the problem of stability in Section 2.

Proving Theorem 1 requires fixing a gauge. This is a mechanism to eliminate the diffeomorphism covariance of (1.1), i.e., the fact that for any diffeomorphism $\phi : \mathcal{M} \to \mathcal{M}$, the pullback $\phi^* g$ is a solution of (1.1) whenever g is. Consider first a local problem in which $\Sigma = B(0,1) \subset \mathbb{R}^3$ is the unit ball, and we aim to construct, in a neighborhood of $i(\Sigma) = \{0\} \times \Sigma \subset \mathcal{M}' := \mathbb{R} \times B(0,1)$, a solution g of (1.1) which induces the data $(\overline{g}, K)$ at the hypersurface $\{0\} \times B(0,1)$. In local coordinates $(t,x) = (z^0, z^1, z^2, z^3)$ on $\mathcal{M}'$, equation (1.2) for the metric $g = (g_{ij})_{1\le i,j\le 4}$ takes the form

$$\begin{aligned}\mathrm{Ric}(g)_{ij} - \Lambda g_{ij} = -\frac{1}{2} g^{k\ell}\partial_k\partial_\ell g_{ij} + \frac{1}{2}\big(\partial_i W_j(z,g,\partial g) + \partial_j W_i(z,g,\partial g)\big) \\ + N_{ij}(z,g,\partial g) = 0 \qquad (1.4)\end{aligned}$$

(with summation over repeated indices), where (g^{ij}) is the matrix inverse of (g_{ij}), furthermore $N_{ij}(z,g,\partial g)$ is a nonlinear expression in the coefficients of g and its first coordinate derivatives, and finally

$$W_i(z,g,\partial g) = g_{i\ell} g^{jk} \Gamma^\ell_{jk},$$

with $\Gamma^i_{jk} = \Gamma^i_{jk}(g)$ denoting the Christoffel symbols of g. Given any *gauge source functions* $F_i = F_i(z,g)$, we then aim to solve equation (1.4) in the *generalized harmonic gauge* $W_i(z,g,\partial g) = F_i(z,g)$. (The special case $F_i = 0$ is the *wave coordinate gauge*.[1]) Inserting this gauge condition into (1.4), one obtains a system of quasilinear wave equations for the metric coefficients g_{ij}, with principal part given by $-\frac{1}{2}\Box_g g_{ij}$. We can write this system in the compact form

$$P(g) := \mathrm{Ric}(g) - \Lambda g - \delta_g^*(W - F) = 0, \qquad (1.5)$$

where $W = W_i \mathrm{d}z^i$ and $F = F_i \mathrm{d}z^i$, and δ_g^* is the symmetric gradient defined by $(\delta_g^*\omega)_{ij} = \frac{1}{2}(\omega_{i;j} + \omega_{j;i})$ where $\omega_{i;j} := (\nabla_{\partial_j}\omega)(\partial_i)$. For future purposes, note that $P(g) = 0$ is a quasilinear wave equation when g is Lorentzian, whether $W - F = 0$ or not. Equation (1.5) is called the *gauge-fixed Einstein (vacuum) equation*.

One now solves the initial value problem in the gauge $W - F = 0$ as follows:

(1) One constructs (algebraically, i.e., without having to solve any differential equation) smooth Cauchy data (g^0, g^1), where $g^\mu = (g^\mu_{ij}(x))$ is a spacetime symmetric 2-tensor (symmetric 4×4 matrix) on Σ, in such a way that $\overline{g}$, resp. K are the induced metric, resp. second fundamental form of $\{0\} \times \Sigma$ induced by any spacetime metric g on $\mathcal{M}'$ with $(g^0, g^1) = (g|_{t=0}, \partial_t g|_{t=0})$. Moreover, the flexibility in the choice of (g^0, g^1) is used to ensure that the gauge condition $W - F = 0$ is satisfied at $t = 0$; the verification of this condition indeed only requires knowledge of the Cauchy data (g^0, g^1).

1 The terminology arises from the fact that $W^i = \Box_g z^i$ where $\Box_g = |g|^{-1/2}\partial_i |g|^{1/2} g^{ij}\partial_j$ is the scalar wave operator. That is, in the wave coordinate gauge, the coordinate functions z^i satisfy the homogeneous wave equation.

(2) One solves the initial value problem $P(g) = 0$, $(g, \partial_t g)|_{t=0} = (g_0, g_1)$ for g. Since this is a quasilinear wave equation, one has local existence and uniqueness of solutions (but solutions may develop singularities in finite time).

(3) The constraint equations (1.3) together with $P(g) = 0$ and $W - F = 0$ at $i(\Sigma)$ can be shown to imply, via a direct computation, that also $\partial_t(W - F) = 0$ at Σ.

(4) The second Bianchi identity is equivalent to the statement that for any metric g, one has $\operatorname{div}_g \mathsf{G}_g \mathrm{Ric}(g) = 0$. Applying $\operatorname{div}_g \mathsf{G}_g$ to equation (1.5) thus produces a decoupled equation for $W - F$,

$$\operatorname{div}_g \mathsf{G}_g \delta_g^*(W - F) = 0.$$

This is a homogeneous wave equation with principal part $-\frac{1}{2}\Box_g(W - F)$. Since $W - F$ has trivial Cauchy data at $i(\Sigma)$, we conclude that $W - F \equiv 0$ in the domain of dependence of $i(\Sigma)$ with respect to the metric g.

(5) Plugging $W - F = 0$ into (1.5) shows that also $\mathrm{Ric}(g) - \Lambda g = 0$ in the same domain.

This argument also shows that solutions of the Einstein vacuum equations obey finite speed of propagation. Thus, passing from local solutions to the maximal Cauchy development can be accomplished by carefully gluing together local solutions.

We point out that different choices of gauge source functions F_i may cause singularities to form at different subsets of spacetime. For controlling the *global* evolution of spacetimes, it is thus of central importance to make a well-informed choice of F_i; there is no known method to make an optimal or even a good choice in general. A particularly geometric choice can be made when $\mathcal{M} = \mathbb{R} \times \Sigma$ is already equipped with a "background metric" g^0: in this case one can take $F_i = g_{i\ell} g^{jk} \Gamma^\ell_{jk}(g^0)$, and the gauge condition $W - F = 0$ is equivalent to the requirement that the pointwise identity map $(\mathcal{M}, g) \to (\mathcal{M}, g^0)$ be a wave map **[93]**.

An attractive feature of (1.5) is that it highlights the principally scalar (albeit tensorial) character of the gauge-fixed Einstein equation. Thus, many aspects of its analysis are no more difficult than for the linear scalar wave equation, while one retains the flexibility to work in particular coordinates, or splittings of the tangent or cotangent bundles, wherever needed. Further aspects of (variants of) (1.5) and of generalized harmonic gauges will be discussed in Section 2.4.2.

1.3. Double null gauge and the characteristic initial value problem

A particularly geometrically adapted gauge to write the Einstein equation in is the *double null gauge*. The idea is to foliate the spacetime by ingoing and outgoing null hypersurfaces which intersect in (spacelike) 2-manifolds. From a physical perspective, one may expect that this will reveal important structure in the equations as gravitational waves propagate along null hypersurfaces. Indeed, the double null gauge has been successfully employed in several seemingly unrelated contexts, for instance, the formation of black holes **[44]**, the stability of black holes (see Section 2.4.1), the theory of impulsive gravitational waves **[153, 154]** and the construction of naked singularities (see Section 3.2).

Let $\mathcal{W} \subset \mathbb{R}^2$ be a nonempty open subset. A double null gauge on a manifold $\mathcal{M} = \mathcal{W} \times \mathbb{S}^2$ is a coordinate system $(u, v, \theta^1, \theta^2)$ such that the metric takes the form

$$g = -4\Omega^2 \mathrm{d}u\,\mathrm{d}v + \not{g}_{AB}(\mathrm{d}\theta^A - b^A\,\mathrm{d}v)(\mathrm{d}\theta^B - b^B\,\mathrm{d}v), \tag{1.6}$$

where Ω is a spacetime function, $b : \mathcal{M} \to T\mathcal{M}$ an $\mathbb{S}^2_{u,v}$-vector and $\not{g}$ the induced metric on the spheres $\mathbb{S}^2_{u,v} = \{(u, v)\} \times \mathbb{S}^2$.[2] We remark that any Lorentzian metric can be locally put into this form by solving the eikonal equation associated with the metric g.

Associated with a double null foliation is a local double null frame given by

$$e_3 = \frac{1}{\Omega}\partial_u, \quad e_4 = \frac{1}{\Omega}(\partial_v + b^A\partial_{\theta^A}), \quad e_A = \partial_{\theta^A}. \tag{1.7}$$

The vectors e_3 and e_4 are null, and the frame satisfies the normalization conditions $g(e_3, e_4) = -2$, $g(e_3, e_A) = 0 = g(e_4, e_A)$, and $g(e_A, e_B) = \not{g}_{AB}$.

Given a double null gauge, one can define Ricci coefficients and curvature components with respect to the above frame (all these are the coefficients of $\mathbb{S}^2_{u,v}$-tensors)

$$\begin{aligned}
\chi_{AB} &= g(\nabla_A e_4, e_B), & \underline{\chi}_{AB} &= g(\nabla_A e_3, e_B), & \eta &= -\frac{1}{2}g(\nabla_{e_3} e_A, e_4),\\
\hat{\omega} &= \frac{1}{2}g(\nabla_{e_4} e_3, e_4), & \underline{\hat{\omega}} &= \frac{1}{2}g(\nabla_{e_3} e_4, e_3), & \underline{\eta} &= -\frac{1}{2}g(\nabla_{e_4} e_A, e_3),\\
\alpha_{AB} &= R(e_A, e_4, e_B, e_4), & \underline{\alpha}_{AB} &= R(e_A, e_3, e_B, e_3), & \beta &= \frac{1}{2}R(e_A, e_4, e_3, e_4),\\
\rho &= \frac{1}{4}R(e_4, e_3, e_4, e_3), & \sigma &= \frac{1}{4}{}^\star R(e_3, e_4, e_4, e_3), & \underline{\beta} &= \frac{1}{2}R(e_A, e_3, e_3, e_4),
\end{aligned}$$

and write out the null-structure equations (which relate the intrinsic and extrinsic geometry of the spacetime foliation) in terms of $\mathbb{S}^2_{u,v}$-tensors; this leads to a system of transport equations along the null cones, and elliptic equations on the spheres. An example of a transport equation is (note that $\alpha, \underline{\alpha}$ are $\not{g}$-traceless as a consequence of the Einstein equations)

$$\not{\nabla}_4\hat{\chi} + (\mathrm{tr}\,\chi)\hat{\chi} - \hat{\omega}\hat{\chi} = -\alpha, \tag{1.8}$$

where $\hat{\chi}$ denotes the $\not{g}$-traceless part of χ and $\not{\nabla}_4$ denotes the projected covariant derivative in the e_4 direction. An example of an elliptic equation is

$$\not{\mathrm{d}}\mathrm{iv}\,\hat{\chi} = -\frac{1}{2}\hat{\chi} \cdot (\eta - \underline{\eta}) + \frac{1}{4}\,\mathrm{tr}\,\chi(\eta - \underline{\eta}) + \frac{1}{2}\not{\nabla}\,\mathrm{tr}\,\chi - \beta, \tag{1.9}$$

where $\not{\mathrm{d}}\mathrm{iv}$ denotes the $\not{g}$-divergence on $\mathbb{S}^2_{u,v}$. The analytical content of the Einstein equations (1.1) is then captured by these structure equations in conjunction with the Bianchi equations, which capture the essential hyperbolicity of (1.1). An example of two such null-decomposed equations is

$$\not{\nabla}_3\alpha + \frac{1}{2}(\mathrm{tr}\underline{\chi})\alpha + 2\underline{\hat{\omega}}\alpha = -2\not{\mathcal{D}}_2^\star\beta - 3\rho\hat{\chi} - 3^\star\hat{\chi}\sigma + \frac{1}{2}(9\eta - 2\underline{\eta})\,\hat{\otimes}\,\beta, \tag{1.10}$$

$$\not{\nabla}_4\beta + 2(\mathrm{tr}\,\chi)\beta - \hat{\omega}\beta = \not{\mathrm{d}}\mathrm{iv}\,\alpha + \eta \cdot \alpha, \tag{1.11}$$

where $\not{\mathcal{D}}_2^\star$ denotes the symmetric traceless part of the covariant derivative $\not{\nabla}$ on $(\mathbb{S}^2_{u,v}, \not{g})$, $\hat{\otimes}$ the symmetric traceless tensor product, and * is the Hodge-star operator.

2 Tensors $\mathbb{S}^2_{u,v}$ can be canonically identified with spacetime tensors having the property that any contraction with the null directions in (1.7) is identically zero.

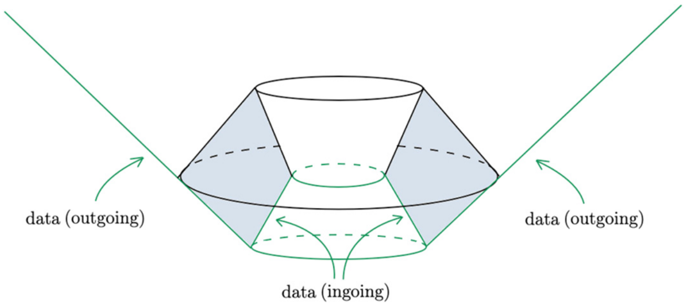

FIGURE 1
The characteristic initial value problem and the double null foliation. Data is specified on the green ingoing and outgoing cones and the solution exists in the grey shaded region.

As mentioned above, given a solution of the Einstein equations, we can locally put the metric into a double null gauge. Conversely, one can *construct* local solutions to the Einstein equations in a double null gauge by solving a characteristic initial value problem, where initial data are prescribed on two intersecting null cones (see Figure 1).

Theorem 2 ([130, 149, 178]). *Consider suitable smooth vacuum initial data prescribed on two (what will be) null hypersurfaces intersecting transversally on a spacelike* 2*-sphere* $S_0 = N_1 \cap N_2$. *Then there exists a nonempty maximum development* $(\mathcal{M}, g)$ *which is bounded in the past by a neighborhood of* S_0 *in* $N_1 \cup N_2$.

The proof of the theorem reduces the problem to the situation of Theorem 1 (the hypersurface S_0 can in fact be any two-dimensional spacelike surface).

As we shall see, the relevance of the double null gauge is most apparent in (semi)-global problems through the way it allows to estimate the solution. We mention explicitly already Luk's result [149] which provides estimates on the size of the corresponding maximum development in Theorem 2 by means of exploiting the null structure in the equations.

We have not given a precise notion of a vacuum initial data set prescribed on intersecting null hypersurfaces in Theorem 2. The definition and the procedure to construct such data can be found in [44]. Roughly speaking, in canonical coordinates (1.6) and using stereographic coordinates on the sphere, the free data correspond to prescribing, in a smooth fashion, a symmetric traceless 2×2-matrix along each of the initial cones as well as the mean curvatures and the torsion at the sphere of intersection. All remaining geometric quantities are then determined by solving ordinary differential equations along the initial cones.

1.4. Explicit solutions

1.4.1. Maximally symmetric solutions

The simplest solution to (1.1) for $\Lambda = 0$ is *Minkowski space* $(\mathbb{R}^4, \eta)$, where $\eta = -\mathrm{d}t^2 + \sum_{j=1}^{3} (\mathrm{d}x^j)^2$ in standard coordinates (t, x^1, x^2, x^3) on $\mathbb{R}^4$. It is geodesically complete and maximally symmetric in that the spacetime admits the maximum number of

Killing vectors, namely 10. These correspond to the infinitesimal generators of the Poincaré group of special relativity (spacetime translations, spatial rotations, Lorentz boosts). Passing to polar coordinates (r, θ, ϕ) on $\mathbb{R}^3$ and denoting by $\mathring{g} = d\theta^2 + \sin^2\theta\, d\phi^2$ the standard metric on $\mathbb{S}^2$, we have

$$\eta = -dt^2 + dr^2 + r^2\mathring{g} = -dU\, dV + r^2(U, V)\mathring{g}, \quad U = t + r,\ V = t - r,$$

with $r(U, V) = \frac{1}{2}(U - V)$, and $(U, V) \in (-\infty, \infty) \times (-\infty, \infty)$ is restricted to the subset where $r(U, V) \geq 0$. Since η is spherically symmetric, we can give a simple description of the causal geometry by depicting the (U, V) plane, compactified at $U = \infty$ and at $V = -\infty$. See Figure 2. The ideal boundary at $U = \infty$, resp. $V = -\infty$, is called *future*, resp. *past null infinity* ($\mathscr{I}^+$, resp. $\mathscr{I}^-$).

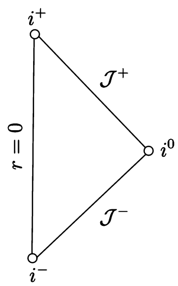

FIGURE 2
Penrose diagram of the Minkowski spacetime.

Certain approaches [116] to the analysis of wave equations on the Minkowski spacetime (or suitable perturbations thereof [18, 19]) instead focus first on the fact that η is homogeneous of degree -2 with respect to scaling in (t, x). Thus, one attaches an ideal boundary at $|(t, x)| = \infty$ by passing to the radial (or projective) compactification $\overline{\mathbb{R}^4}$ of $\mathbb{R}^4$, which is a closed 4-ball. All forward light cones intersect the ideal boundary in the same 2-sphere (analogously for backward light cones). Resolving these by means of real blow-up produces, as front faces, future and past null infinity. The resulting manifold with corners can also be regarded as a blow-up of the Penrose diagram at i^0 and $i^\pm$, see Figure 3.

The maximally symmetric analogue of Minkowski space for $\Lambda > 0$ is called *de Sitter space*. This can be defined as the cylinder

$$\mathcal{M} = \left(-\frac{\pi}{2}, \frac{\pi}{2}\right)_s \times \mathbb{S}^3, \quad g = \Omega^{-2}\overline{g}, \quad \Omega^2 = \frac{\Lambda}{3}\cos^2 s, \quad \overline{g} = -ds^2 + g_{\mathbb{S}^3}. \quad (1.12)$$

The boundary at $s = \pm\frac{\pi}{2}$ is called the *future/past conformal boundary*. Since null-geodesics of conformally related metrics are the same up to reparametrization, the causal structure of $(\mathcal{M}, g)$ is the same as that of $\mathcal{M}$ equipped with the smooth (down to $s = \pm\frac{\pi}{2}$) metric $\overline{g}$. See Figure 4.

Due to the finite speed of propagation for solutions of wave equations, one can consider wave equations in a *static patch of de Sitter space*, which is the intersection of the

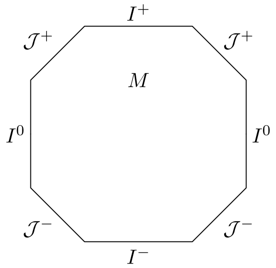

FIGURE 3
Resolution (blow-up) of the radial compactification $\overline{\mathbb{R}^4}$.

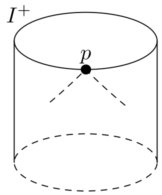

FIGURE 4
(Global) de Sitter space. Also shown is part of the backwards light cone from a point p on the future conformal boundary I^+.

timelike past of a point $p = (\frac{\pi}{2}, q)$ and the timelike future of $(-\frac{\pi}{2}, q)$. One can introduce coordinates in such a domain in which the de Sitter metric is static,

$$g = -\left(1 - \frac{\Lambda}{3}r^2\right)\mathrm{d}t^2 + \left(1 - \frac{\Lambda}{3}r^2\right)^{-1}\mathrm{d}r^2 + r^2\mathring{\not{g}}. \tag{1.13}$$

The singularity of this expression at the *cosmological horizon* $r^{-1}(\sqrt{3/\Lambda})$ (which in $s > 0$ is the backwards light cone with vertex p) is a coordinate singularity.

Finally, the maximally symmetric spacetime with $\Lambda < 0$ is called anti-de Sitter space (AdS). This is the manifold $\mathbb{R}^4$ equipped with the metric (1.13) where now $\Lambda < 0$. Using the transformation $r = \tan\psi$ (with $\psi \in (0, \pi/2)$) the metric (1.13) can be written as $g = \frac{1}{\cos^2\psi}(-dt^2 + d\psi^2 + \sin^2\psi\,\mathring{\not{g}})$ from which it becomes apparent that AdS is conformal to $\mathbb{R} \times \mathbb{S}^3_h \subset \mathbb{R} \times \mathbb{S}^3$ ($\mathbb{S}^3_h$ denoting a hemisphere of $\mathbb{S}^3$), equipped with the metric $-dt^2 + g_{\mathbb{S}^3}$, i.e., conformal to one "half" of the Einstein static cylinder. The timelike boundary $\psi = \frac{\pi}{2}$ in the conformal picture corresponds to the timelike *conformal infinity* ($r = \infty$) of anti-de Sitter space. The spacetime is not globally hyperbolic and boundary conditions will have to be imposed to get a well-posed evolution for hyperbolic equations on or near these backgrounds. See Figure 5.

1.4.2. The Schwarzschild manifold

A nontrivial solution to the Einstein equations was found by Schwarzschild in 1915. The Schwarzschild solution describes what we (today) call a black hole solution. We follow a

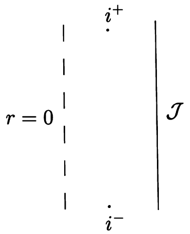

FIGURE 5
The Penrose diagram of anti-de Sitter space with its timelike conformal boundary $\mathcal{I}$.

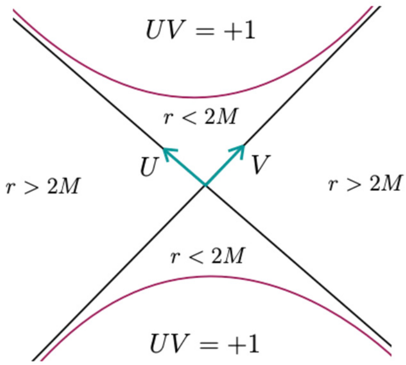

FIGURE 6
The causal geometry of the maximally extended Schwarzschild manifold.

somewhat revisionist approach in presenting the metric which however emphasizes directly its geometric nature and its connection to the double null gauge introduced in Section 1.3.

Given $M > 0$, equip $\mathcal{M} = (-\infty, \infty)_U \times (-\infty, \infty)_V \times \mathbb{S}^2 \cap \{UV < 1\}$ with the metric

$$g_M = -4\Omega_K^2 \mathrm{d}U\, \mathrm{d}V + r^2(U,V)\mathring{\slashed{g}}, \quad \Omega_K^2 = \frac{8M^3}{r}\exp\Big(-\frac{r}{2M}\Big),$$

where $r : (-\infty, \infty) \times (-\infty, \infty) \to \mathbb{R}^+$ is defined implicitly by

$$\Big(\frac{r(U,V)}{2M} - 1\Big)\exp\Big(\frac{r(U,V)}{2M}\Big) = -UV.$$

We time-orient $(\mathcal{M}, g_M)$ by declaring $\partial_U + \partial_V$ to be future directed. The metric is spherically symmetric, and we can give a simple depiction of the causal geometry by depicting the (U,V)-plane below. We observe that for the region $U < 0$, $V > 0$ we must have $r < 2M$; moreover, any future directed curve causal curve emanating from this region remains in this region, has finite affine length, and terminates on the asymptotic boundary $UV = 1$, where $r \to 0$ and the Kretschmann scalar $R_{\mu\nu\sigma\nu}R^{\mu\nu\sigma\nu}$ blows up like r^{-6}. It follows that the spacetime is geodesically incomplete and $\mathcal{C}^2$-inextendible (in fact, $\mathcal{C}^0$-inextendible [188]) as a Lorentzian manifold. One may compactify the U and the V coordinates to produce the well-known Penrose-diagram of the Schwarzschild metric, see Figures 6 and 7.

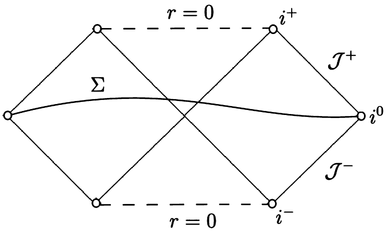

FIGURE 7
Penrose diagram of the Schwarzschild manifold.

The set $r = \infty$ is now realized as a (null) boundary of the spacetime, and we can define the black hole region as $\mathcal{M} \setminus J^{-}(\mathcal{J}^{+})$, i.e., as the set of observers that cannot communicate with asymptotic observers in the far away region of spacetime. The black hole region is bounded by the set $r^{-1}(2M)$, which is a union of null hypersurfaces.

We finally note that if we restrict to the black hole exterior region $U > 0$, $V > 0$, then the sequence of coordinate transformations $U = -e^{-\frac{u}{2M}}$, $V = e^{\frac{v}{2M}}$, $u = \frac{t-r^\star}{2}$, $v = \frac{t+r^\star}{2}$, where $\frac{dr^\star}{dr} = \frac{1}{1-\frac{2M}{r}}$, brings the metric into the standard (static) form where the area radius r is used as a coordinate:

$$g = -\left(1 - \frac{2M}{r}\right)\mathrm{d}t^2 + \left(1 - \frac{2M}{r}\right)^{-1} \mathrm{d}r^2 + r^2 \mathring{g}. \tag{1.14}$$

This coordinate system breaks down when r equals the Schwarzschild radius $r = 2M$; coordinates valid across $r = 2M$ (besides the Kruskal coordinates U, V above) are discussed in Section 1.4.3. Expression (1.14) shows that the Schwarzschild metric is stationary (∂_t is a Killing vector field and timelike for large r, or indeed for all $r > 2M$).

An important feature of the Schwarzschild metric and other black hole spacetimes discussed below is the existence of *trapped null-geodesics* in the exterior region $r > 2M$, i.e., future and past inextendible null-geodesics which when quotienting out by time translations (i.e., projecting to the (r, θ, ϕ) variables) remain in a compact subset of $\{r > 2M\}$. The trapped set is defined as the subset of phase space $T^*\mathcal{M}$ consisting of all (z, ζ) so that the null-geodesic with initial position z and initial momentum $\zeta \in T^*\mathcal{M}$, $\zeta \neq 0$, is trapped. Writing

$$\zeta = \sigma\,\mathrm{d}t + \xi\,\mathrm{d}r + \eta, \quad \eta \in T^*\mathbb{S}^2,$$

the trapped set of the Schwarzschild spacetime is the conic set

$$\Gamma = \left\{\zeta \in T^*\mathcal{M} \setminus o : r = 3M, \xi = 0, |\eta|^2_{\mathring{g}^{-1}} = 27M^2\sigma^2\right\}. \tag{1.15}$$

Its projection to the base manifold $\mathcal{M}$ is the hypersurface $r = 3M$. The trapped set is unstable, and indeed ν-normally hyperbolic for all ν **[118]**, as will be discussed in more detail in Section 2.3.4.

We finally mention the important *red-shift effect* **[171]**, which is in fact a general feature of nondegenerate black hole horizons. In the geometric optics approximation, it manifests itself by the frequency of waves (measured with respect to an appropriate notion of time) being shifted towards longer (i.e., less energetic) frequencies as they propagate near the event horizon. For hyperbolic equations, the red-shift effect can be captured by a physical space energy identity with good coercive properties near the horizon [63]. From the viewpoint of microlocal analysis these are the radial estimates of [201] (see Section 2.3.4).

1.4.3. Further spherically symmetric spacetimes

The Schwarzschild solution generalizes to the Reissner–Nordström–((anti)-de Sitter) solution of the Einstein–Maxwell equations with cosmological constant (1.1) (we omit the explicit formulas for the electromagnetic field here). The line element in so-called static coordinates is

$$g = -\left(1 - \frac{2M}{r} + \frac{Q^2}{r^2} - \frac{\Lambda}{3}r^2\right)dt^2 + \left(1 - \frac{2M}{r} + \frac{Q^2}{r^2} - \frac{\Lambda}{3}r^2\right)^{-1} dr^2 + r^2\mathring{g}. \quad (1.16)$$

Near the zeros of $F(r) = 1 - \frac{2M}{r} + \frac{Q^2}{r^2} - \frac{\Lambda}{3}r^2$, one needs to pass to other coordinate systems to unravel the maximally extended spacetimes shown in the Penrose diagrams below. For instance, near the event horizon $r = r_+$ where F changes sign from $-$ to $+$, one can introduce ingoing Eddington–Finkelstein coordinates, $v = t + \int F^{-1}\,\mathrm{d}r$, in which

$$g = -F(r)\,\mathrm{d}v^2 + 2\,\mathrm{d}v\,\mathrm{d}r + r^2\mathring{g}.$$

For $\Lambda = 0$ but nonzero subextremal charge $0 \neq |Q| < M$, the Penrose diagram of the Reissner–Nordström spacetime differs dramatically from that of the Schwarzschild spacetime in the black hole region: while there still is an event horizon at $r = r_+ := M + \sqrt{M^2 - Q^2}$, there is now also a future/past *inner horizon* (or *Cauchy horizon*) at $r = r_- := M - \sqrt{M^2 - Q^2}$ across which the metric extends analytically. The Cauchy horizon is the boundary of the maximal Cauchy development of the initial data at the hypersurface Σ indicated in Figure 8. For $\Lambda > 0$ and $Q = 0$, the metric (1.16) is a vacuum

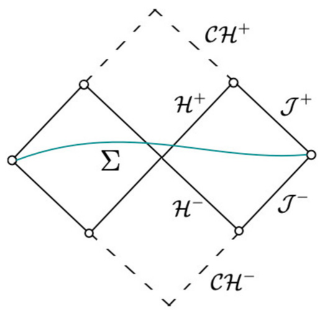

FIGURE 8
A piece of the maximal analytic extension of the Reissner–Nordström spacetime.

solution of (1.1) and called the Schwarzschild–de Sitter (SdS) metric; we consider only the subextremal case $0 < 9M\Lambda^2 < 1$. Its geometry near the black hole and near the event horizon $r = r_-$ (the smaller positive root of $1 - \frac{2M}{r} - \frac{\Lambda}{3}r^2 = 0$) is then the same as for the

Schwarzschild metric, but now there is also a second horizon, called *cosmological horizon*, at the larger positive root $r = r_+$ of $1 - \frac{2M}{r} - \frac{\Lambda}{3}r^2 = 0$; this is analogous to the cosmological horizon of the static patch of de Sitter space. The metric extends analytically past this horizon and asymptotes to the de Sitter metric as $r \to \infty$. See Figure 9.

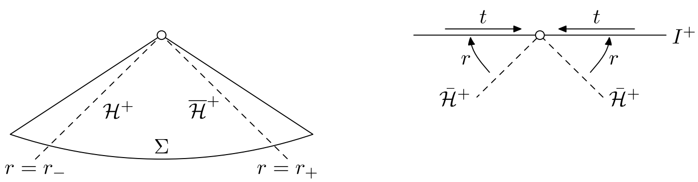

FIGURE 9
(Left) Penrose diagram of a neighborhood $r_- - \varepsilon < r < r_+ + \varepsilon$ of the domain of outer communications of a subextremal Schwarzschild–de Sitter (SdS) spacetime near the causal future of a hyperboloidal spacelike slice Σ. (Right) An illustration of a SdS black hole with a focus on its asymptotically de Sitter geometry far from the black hole; $\overline{\mathcal{H}^+}$ denotes the cosmological horizon.

The (subextremal) Reissner–Nordström–de Sitter spacetime has an event horizon and a cosmological horizon just like the Schwarzschild–de Sitter spacetime. Only the structure of the black hole interior depends on whether $Q = 0$ (in which case there is a terminal singularity as in the Schwarzschild case) or $Q \neq 0$ (in which case there is a Cauchy horizon across which the metric extends analytically).

For $\Lambda < 0$ and $Q = 0$, the metric (1.16) is a vacuum solution of (1.1) and called the Schwarzschild–anti-de Sitter metric. Its crucial geometric features are the timelike conformal boundary at infinity (which is future complete) and the future complete event horizon located at the unique real zero of $F(r)$.

All these spherically symmetric black hole spacetimes have trapped sets of the same form as (1.15), with $3M$ and $27M^2$ replaced by appropriate constants.

1.4.4. The Kerr metric and related metrics

In 1963 Roy Kerr found a generalization of the Schwarzschild family of metrics to a family of vacuum solutions of (1.1) (with $\Lambda = 0$) which incorporates also angular momentum. For parameters $M > 0$ and $a \in [-M, M]$, and setting $r_+ = M + \sqrt{M^2 - a^2}$, the *Kerr family of metrics*, in Boyer–Lindquist coordinates $t \in \mathbb{R}$, $r \in (r_+, \infty)$, $\theta \in (0, \pi)$, $\phi \in (0, 2\pi)$, takes the form

$$g_{M,a} = -\frac{\Delta}{\varrho^2}(\mathrm{d}t - a\sin^2\theta\,\mathrm{d}\phi)^2 + \varrho^2\left(\frac{\mathrm{d}r^2}{\Delta} + \mathrm{d}\theta^2\right) + \frac{\sin^2\theta}{\varrho^2}\big(a\,\mathrm{d}t - (r^2 + a^2)\,\mathrm{d}\phi\big)^2,$$
$$\Delta = r^2 - 2Mr + a^2, \quad \varrho^2 = r^2 + a^2\cos^2\theta. \tag{1.17}$$

For $a = 0$, this reduces to (1.14).

For now, we focus on the *subextremal range* $a \in (-M, M)$. For $a \neq 0$, the Penrose diagram of suitable two-dimensional timelike slices of the maximal analytic extension of the Kerr spacetime has the same form as that of the Reissner–Nordström spacetime, see Figure 8. In particular, there is an event horizon at $r = r_+$ and a Cauchy horizon at $r = r_- := M - \sqrt{M^2 - a^2}$.

Furthermore, there is a trapped set Γ, which as in the Schwarzschild case is a smooth (in fact, analytic) conic submanifold $\Gamma \subset T^*\mathcal{M} \setminus o$ of phase space over the black hole exterior $r > r_+$; it is an ν-normally hyperbolic (for every ν) invariant submanifold for the lift of the null-geodesic flow to $T^*\mathcal{M}$, as first noted by Wunsch–Zworski [210] and proved in the full subextremal range by Dyatlov [76]. The projection of Γ to the base $\mathcal{M}$ is however no longer a smooth submanifold, but rather a full-dimensional closed set (with compact intersection with any t-level set) with non-empty interior.

Another novel feature of rotating Kerr metrics is the presence of *superradiance*. This means that the energy $-g_{M,a}(\dot\gamma, \partial_t)$ of a future lightlike geodesic γ with respect to the generator ∂_t of time translations may be *negative*; here ∂_t is the unique (up to scaling) Killing vector field which for sufficiently large r/M is future timelike. This is the basis of the Penrose effect for energy extraction from rotating black holes. On the level of analysis, this problem is overcome by means of so-called red-shift or radial point estimates.

We mention a geometric and an algebraic fact about the Kerr metric. Firstly, there exists a global double null foliation on the Kerr manifold (constructed in [174]). Secondly, there exists a (nonintegrable) null-frame, called the algebraically special frame, on the Kerr manifold with respect to which all but the curvature components ρ and σ (defined as in Section 1.3 but for the null frame being the algebraically special frame) vanish.

Finally, we note that for *extremal Kerr black holes*, with $|a| = M$, the event horizon at $r = M$ degenerates (the function Δ in (1.17) has a double zero). Furthermore, the trapped set now extends down to the horizon and ceases to be normally hyperbolic [76].

The generalization of (1.17) allowing for the presence of a cosmological constant Λ and an electric charge Q was found by Carter [36], following the discovery [170] of the charged analogue in the case $\Lambda = 0$. It is called the Kerr–Newman–((anti)-de Sitter) metric,

$$
\begin{aligned}
g_{M,a,\Lambda,Q} &= -\frac{\Delta}{(1+\lambda)\varrho^2}(\mathrm{d}t - a\sin^2\theta\,\mathrm{d}\phi)^2 + \varrho^2\left(\frac{\mathrm{d}r^2}{\Delta} + \frac{\mathrm{d}\theta^2}{\kappa}\right) \\
&\quad + \frac{\kappa\sin^2\theta}{(1+\lambda)^2\varrho^2}\big(a\,\mathrm{d}t - (r^2+a^2)\,\mathrm{d}\phi\big)^2, \\
\lambda &= \frac{\Lambda}{3}a^2, \quad \kappa = 1 + \lambda\cos^2\theta, \quad \varrho^2 = r^2 + a^2\cos^2\theta, \\
\Delta &= (r^2+a^2)\left(1 - \frac{\Lambda}{3}r^2\right) - 2Mr + (1+\lambda^2)Q^2.
\end{aligned}
\tag{1.18}
$$

(We again omit the explicit expression for the electromagnetic field.) For $Q = 0$ and $\Lambda > 0$ ($\Lambda < 0$), this is called the Kerr–(anti-)de Sitter metric. For simplicity, in these notes we restrict attention to the case of small angular momenta a and small charges Q; in this case, the Penrose diagram of suitable two-dimensional slices of a neighborhood of the black hole exterior region of Kerr–Newman–de Sitter spacetimes is the same as the one of a SdS spacetime, as shown in Figure 9. Again, there is a trapped set with the same (phase space and physical space) structure as in the subextremal Kerr case.

1.5. Matter models

In the notation of equation (1.1), we have so far restricted ourselves to the vacuum case $\mathbb{T} = 0$. However, real world physical systems typically involve matter. We briefly discuss the most common matter models studied in connection with the Einstein equations. In each of these cases, the stated expression for $\mathbb{T}$ arises by direct calculation from the Euler–Lagrange equation for a suitable Lagrangian (the Einstein–Hilbert action plus additional terms describing the matter).

For real-valued *scalar fields* ϕ with mass m, one takes

$$\mathbb{T}_{\mu\nu} = (\partial_\mu\phi)(\partial_\nu\phi) + m^2\phi^2 - \frac{1}{2}g_{\mu\nu}|\nabla\phi|_g^2. \tag{1.19}$$

The second Bianchi identity implies that for a solution of (1.1) with this energy–momentum tensor, ϕ necessarily solves the Klein–Gordon equation (for $m = 0$ the wave equation)

$$(\Box_g - m^2)\phi = 0.$$

For *electromagnetic fields* $F = F_{\mu\nu}\mathrm{d}x^\mu \wedge \mathrm{d}x^\nu$, one takes

$$\mathbb{T}_{\mu\nu} = g^{\alpha\beta}F_{\alpha\mu}F_{\beta\mu} - \frac{1}{4}F^{\alpha\beta}F_{\alpha\beta}g_{\mu\nu}. \tag{1.20}$$

The second Bianchi identity gives as the equations of motion the Maxwell equations

$$\mathrm{d}F = 0, \quad \mathrm{div}_g\, F = 0.$$

On spacetimes with nonzero electromagnetic fields $F = \mathrm{d}A$, one can also consider *charged scalar fields*; they are sections of a complex line bundle satisfying a wave equation defined with respect to the connection $\mathrm{d} - iA$.

Finally, uncharged collisionless ("Vlasov") matter with mass $m \geq 0$ is described by a density distribution $f : T\mathcal{M} \to [0,\infty)$ with support in the set of future causal v with $g(v,v) = -m^2$; the energy–momentum tensor at the point $p \in \mathcal{M}$ is

$$\mathbb{T}_{\mu\nu}(p) = \int_{T_p\mathcal{M}} f(p,v)v_\mu v_\nu, \quad v_\mu = g_{\mu\nu}v^\nu. \tag{1.21}$$

The equation of motion for the density f is the transport equation $Xf = 0$, where X is the geodesic vector field on $T\mathcal{M}$.

2. THE STABILITY OF BLACK HOLE SOLUTIONS

Before we turn to the discussion of the stability of the black hole solutions (described in Section 1.4) in Section 2.2, we record what is known about the stability of the maximally symmetric solutions.

2.1. Prelude: stability of maximally symmetric solutions

The sign of the cosmological constant has a dramatic effect on the global structure of the maximally symmetric solutions, and thus we discuss the three cases separately.

2.1.1. $\Lambda = 0$

For $\Lambda = 0$, we have the following seminal result:

Theorem 3 ([45]). *Minkowski spacetime* $(\mathbb{R}^4, \eta)$ *is nonlinearly asymptotically stable.*

We note earlier work of Friedrich [87] proving a version of the above theorem for initial data which are exactly Schwarzschildean outside a compact set (such data were later constructed in [47,48]) or prescribed on a hyperboloidal slice ending at null infinity.

While the original proof of Theorem 3 is closer in spirit to the analysis of the equations in double null form (in particular, [45] estimates curvature and Ricci coefficients instead of metric components), a simplified proof of the theorem (with weaker conclusions regarding the asymptotics) was later given in harmonic gauge by Lindblad–Rodnianski [146].

Studying the stability of flat space is still an active area of research with many new developments regarding regularity [23], optimal asymptotic decay rates [116,145], and coupling to various matter models. A particularly interesting direction is to consider flat space as a solution to the (massive or massless) Einstein–Vlasov system. Unlike for the scalar field or electromagnetic radiation, the matter does not satisfy wave-type equations but instead transport equations (see Section 1.5). This requires a several new ideas including the construction of various lifts of geometrically adapted vector fields to the mass-shell to identify a suitable version of the null condition in the nonlinearities. In summary we have:

Theorem 4 ([24,79,147,199]). *Minkowski spacetime* $(\mathbb{R}^4, \eta)$ *is nonlinearly asymptotically stable as a solution of the coupled Einstein–Vlasov system.*

2.1.2. $\Lambda > 0$

The first general nonlinear stability result for the Einstein vacuum equations was obtained for perturbations of de Sitter space $(-\frac{\pi}{2}, \frac{\pi}{2})_s \times \mathbb{S}^3$ by Friedrich [87]: the metric evolving from small and sufficiently regular perturbations of de Sitter initial data at $\Sigma = \{s = 0\}$ can be written as $\Omega^{-2}\overline{g}$ where Ω is positive near Σ and vanishes simply at what becomes the future and past conformal boundary, cf. (1.12). (Thus, the spacetime is *not* asymptotic to de Sitter spacetime as $\Omega \searrow 0$.) Moreover, such asymptotically de Sitter spacetimes can be characterized via suitable asymptotic initial data (two scalar functions and a symmetric 2-tensor K on a Riemannian 3-manifold $(\mathbb{S}^3, h)$) at the future conformal boundary which satisfy *linear* constraint equations (K must be trace- and divergence-free). See Section 4.1 for a recent result making use of this fact on a conceptual level. Extensions of [87] to general dimensions were proved in [4,179]. A different perspective on the stability of small neighborhoods of the static patch of de Sitter space (in generalized harmonic gauges) was given in [115], see also Section 2.5.2 below.

2.1.3. $\Lambda < 0$

The least understood case is $\Lambda < 0$. Here the Einstein equations become a nonlinear initial boundary value problem for which well-posedness was established in [88]. The question of global stability or instability depends on the boundary conditions imposed at the conformal boundary. The most interesting case are reflective boundary conditions as they preclude any mechanism for energy to be radiated away. (In the case of dissipative boundary conditions, [119] established strong decay for the linearized problem.) The fact that linear fields do not decay lead [55] to conjecture the nonlinear instability of AdS. The problem was first investigated heuristically and numerically for the spherically symmetric scalar field in the influential [25] which proposed a mechanism of energy transfer from low to high frequencies based on resonant interactions. After a large body of works in the theoretical physics literature (see [17, 53, 69] and also the discussion and references in [169]) trying to extend the range of validity of non-linear perturbation theory, Moschidis succeeded in proving the following result:

Theorem 5 ([169]). *Anti-de Sitter spacetime is dynamically unstable as a solution to the spherically symmetric Einstein–Vlasov system.*

The proof proceeds by constructing a one-parameter family of initial data $\mathcal{D}^{\varepsilon}$, consisting of a collection of carefully arranged (both in physical and in momentum space) Vlasov beams, which converges in a suitable topology to the trivial (anti-de Sitter) data as $\varepsilon \to 0$ and is such that for all $\varepsilon > 0$ the maximum development contains a black hole region. Hence, remarkably, (the proof of) Theorem 5 controls the dynamics all the way to the formation of a black hole!

The proof discovers and exploits a nonlinear growth mechanism in physical space (which has no linear analogue and is quite different from the heuristic mechanisms based on resonances for nonlinear perturbations) which relies on the observation that the beams transfer energy to one another when they pass through each other and that this transfer depends on where in spacetime the interaction happens. This observation is at the root of constructing the initial configuration of the beams.

The next natural step is to generalize Theorem 5 to the spherically symmetric Einstein scalar field system. A proof of singularity formation for the Einstein vacuum equation without symmetry assumptions may then be well within reach; this would complete the picture of the vacuum (in)stability of the maximally symmetric solutions.

We finally remark that it is not clear whether instability holds for all (small) data. The existence of geons and "islands of stability" has been widely discussed in the physics literature [94, 122, 184]. For the problem of constructing small data time-periodic solutions in this setting mathematically rigorous progress has recently been made (for semilinear toy problems) in [1].

2.2. The formulation of the stability problem and overview of the results

To formulate the exterior stability problem for black holes it will be useful to distinguish informally the following concepts:[3]

3 These concepts can be modified in a straightforward manner so that they apply for $\Lambda > 0$ or $\Lambda < 0$ as well.

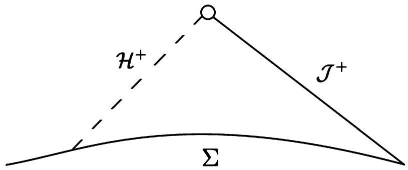

FIGURE 10
Penrose diagram of a (dynamical) black hole spacetime.

(1) *Nonlinear stability:* Given suitable (i.e., characteristic or spacelike and of sufficient regularity) initial data near those of a member of the Kerr family, the associated maximum development $(\mathcal{M}, g)$ has the following properties:

  (i) It contains a subset of the form given in Figure 10. In particular, future null-infinity $\mathcal{I}^+$ is complete and $J^-(\mathcal{I}^+)$ is bounded to the future by a regular future complete event horizon $\mathcal{H}^+$.

  (ii) Orbital stability (g remains close to $g_{M,a}$ on $\mathcal{M}'$).

  (iii) Asymptotic stability ($g \to g_{\tilde{M},\tilde{a}}$ with $|M - \tilde{M}| < \varepsilon$, $|a - \tilde{a}| < \varepsilon$ as an appropriate notion of time goes to infinity).

(2) *Linear stability:* Linearize equations (1.1) in the metric g around a fixed member of the Kerr family; this produces the equations of linearized gravity. Given suitable initial data for this linearized system, prove that, in a suitable gauge, solutions remain bounded (orbital stability) and indeed decay in time to a linearized (in the parameters (M, a)) Kerr metric (asymptotic stability) on the black hole exterior.

(3) *Toy stability:* Given suitable initial data for the toy problem $\Box_{g_{M,a}} \psi = 0$, prove that solutions remain bounded (orbital stability) and decay in time (asymptotic stability) on the black hole exterior.

While the seminal works in the physics literature, starting with [177], concern aspects of the linear stability problem, the first rigorous theorems are due to Wald and Kay [133,207] on toy stability. The results on toy stability have reached a rather complete state in the past decade; this is the content of Section 2.3. With the conceptual and technical insights thus gained, linear and nonlinear black hole stability problems have become accessible, at least in the case $\Lambda \geq 0$, in the past five years. We discuss the current state of knowledge regarding linear stability in Section 2.4, and regarding nonlinear stability in Section 2.5.

2.3. Toy stability

The following theorem summarizes the picture that has been obtained for the analysis of the toy problem in the various black hole geometries.

Theorem 6. *Consider a solution to the scalar wave equation*

$$\Box_{g_{M,a,\Lambda}}\psi = 0 \tag{2.1}$$

on the black hole exterior of a Kerr–((A)dS) spacetime arising from suitable initial data (and, in the Kerr–AdS case, with Dirichlet boundary conditions at the conformal boundary). Then

(1) *If* $\Lambda > 0$ *and* $|a| \ll M$ *then* ψ *decays exponentially in time to a constant* [73].

(2) *If* $\Lambda = 0$ *and* $|a| < M$ *then* ψ *decays inverse polynomially in time* [66]. *(See Theorem 7 below for the extremal case* $|a| = M$*.)*

(3) *If* $\Lambda < 0$ *and the parameters* (M, a, Λ) *satisfy the Hawking–Reall bound then* ψ *decays logarithmically in time* [120].

There are three main geometric phenomena associated with black holes that are directly relevant for understanding the global behavior of hyperbolic equations on black hole backgrounds and which play a crucial role in the proof of Theorem 6. These are (see the discussion in Section 1.4.4):

(1) the red-shift effect;

(2) the presence of trapped null geodesics;

(3) superradiance.

While the above phenomena are present for all black hole geometries discussed in Section 1.4.4, their strength, coupling, and the large scale geometry of the underlying spacetime lead to the quite different dynamical behaviors exhibited by Theorem 6. We provide a short discussion of these phenomena and how they enter the proof of Theorem 6.

2.3.1. $\Lambda = 0$. The classical vector field approach

In the simplest case $\Lambda = 0$, $a = 0$, the phenomenon of superradiance is absent and the problem can be entirely understood in physical space. As mentioned at the end of Section 1.4.2, the trapped geodesics are all concentrated at $r = 3M$, and one may prove (using appropriate multipliers) the following two estimates [26, 27, 63]:

$$\mathbb{E}[\psi](\tau) \le \mathbb{E}[\psi](0) \quad \text{for all } \tau \ge 0 \quad \text{(boundedness)}, \tag{2.2}$$

$$\mathbb{I}_{\mathrm{deg}}[\psi](\tau_1, \tau_2) \le \mathbb{E}[\psi](0) \quad \text{for all } \tau_2 \ge \tau_1 \ge 0 \quad \text{(local integrated energy decay)}, \tag{2.3}$$

where

$$\mathbb{E}[\psi](\tau) = \int_{\Sigma_{t^\star}} (\partial_{t^\star}\psi)^2 + \left(1 - \frac{2M}{r}\right)(\partial_r\psi)^2 + |\nabla\!\!\!/\,\psi|^2$$

$$\mathbb{I}_{\mathrm{deg}}[\psi](\tau_1, \tau_2) = \int_{\tau_1}^{\tau_2} d\tau \int_{\Sigma_\tau} \frac{1}{r^3}\Bigg[(R^\star\psi)^2 + \left(1 - \frac{3M}{r}\right)^2 \times \left((\partial_{t^\star}\psi)^2 + \left(1 - \frac{2M}{r}\right)(\partial_r\psi)^2 + |\nabla\!\!\!/\,\psi|^2\right)\Bigg].$$

These energies are defined in $(t^\star, r, \theta, \phi)$ coordinates in which the Schwarzschild metric takes the regular form $g = -(1 - \frac{2M}{r})(\mathrm{d}t^\star)^2 + \frac{4M}{r}\mathrm{d}t^\star \mathrm{d}r + (1 + \frac{2M}{r})\mathrm{d}r^2 + r^2 \mathring{\not{g}}$. Furthermore, Σ_τ denotes a slice (which intersects the horizon) of constant τ, and $R^\star = \frac{2M}{r}\partial_t + (1 - \frac{2M}{r})\partial_r$.

The degeneration at $r = 3M$ in the estimate (2.3) is necessary (although it can be weakened to logarithmic degeneration using microlocal techniques) and a manifestation of the trapped null geodesics. The red-shift effect allows one to eliminate the degeneration at $r = 2M$ for the transversal (∂_r in these coordinates) derivatives in (2.2) and (2.3) and can be realized as a physical space multiplier. From the resulting nondegenerate version of the estimates (2.2) and (2.3) one can prove, using a very general physical space method that merely uses the asymptotically flatness of the spacetimes (introduced in **[65]**, see also **[168]**) inverse polynomial decay rates for the solutions which are in particular sufficiently strong for nonlinear applications.

For $\Lambda = 0$, $|a| \ll M$, superradiance is present and the Killing field ∂_t will not produce a coercive energy on spacelike slices. The naive estimate (2.2) fails as energy associated with the vector field ∂_t on a later slice can be larger than that of the initial slice. Moreover, trapped null geodesics now exist on a set of full measure (near $r = 3M$) in spacetime. The estimate (2.3) fails and it is not clear how to prove the required analogue. One approach—which was also the one that was later generalized to the full subextremal case—was to use the separability of equation (2.1) on Kerr and to exploit the fact that when one looks at pieces of the solution supported on certain (angular and time) frequencies, then good uniform estimates can be proven from the ordinary differential equations governing the behavior of the frequency localized components. It is a *tour de force* to construct these frequency localized multipliers which typically exploit a smallness parameter arising from the definition of the frequency regimes. A key insight is that superradiance can be controlled by the red-shift effect. Summing the estimates and the fact that the solution is a priori not L^2 in time provide further technical challenges. See **[64]**. Decay in the case $|a| \ll M$ was also proved in **[198]** by means of pseudodifferential multipliers near the trapped set and in **[6]** by exploiting the second order Carter symmetry operator (related to a hidden symmetry of the spacetime not related to Killing vector fields).

Two additional insights lead to a treatment of the full subextremal case $\Lambda = 0$, $|a| < M$ in **[66]**. The first was that, in the frequency decomposition of the solution outlined above, frequency triples that are affected by superradiance are nontrapped. Thus these two obstacles for decay happen to be disjoint when viewed in frequency space (this breaks down precisely in the extremal case $|a| = M$). The second was a quantitative version of mode stability for the wave equation established in **[193]** which allowed one to treat the range of bounded frequencies (where roughly speaking no smallness factor is available). This also allowed one to estimate precisely the amount of amplification of the solution through the mechanism of superradiance, see also **[67]**.

2.3.2. $\Lambda = 0$: the extremal case

We have

Theorem 7 ([15]). *Consider a solution to the scalar wave equation*

$$\Box_{g_{M,a=M}} \psi = 0 \tag{2.4}$$

on the black hole exterior of an extremal Kerr spacetime. Then axisymmetric ψ decay inverse polynomially in time. However, along the event horizon $\mathcal{H}^+$ higher transversal derivatives of ψ generically grow in time (Aretakis instability).

Theorem 7 was first proved for the spherically symmetric extremal Reissner–Nordström metric in [13, 14] (without the restriction on axisymmetric solutions). The main difficulty is that the aforementioned red-shift effect degenerates and one cannot remove the degeneration at the horizon in the estimates. In fact, there are conservation laws on the event horizon $\mathcal{H}^+$ (discovered by Aretakis) which constitute direct obstructions to decay.

In the case of extremal Kerr, the problems of degenerate red-shift, trapping and superradiance are now fully coupled and cannot be studied separately even at the frequency decomposed level. This is the reason why the global behavior of solutions is only understood for axisymmetric solutions (which are not subject to superradiance). The general case is an open problem that has received a lot of attention from both theoretical physics (see, for instance, [37]) and mathematics recently and is expected to exhibit additional instabilities. See also [1, GAJIC] for recent work in this direction.

2.3.3. $\Lambda = 0$: sharp asymptotics

It is a natural question to ask about the precise decay rates in Theorem 6(2). This problem has a long tradition in the physics literature going back to work of Price [175, 176], with refinements given in [99]. While this question is interesting in its own right, lower bounds on the decay rate directly inform the behavior of solutions in the black hole interior (see Section 3.1 below). The following result is the current state-of-the-art.

Theorem 8 ([11, 106]). *Consider a solution to the scalar wave equation*

$$\Box_{g_{M,a}} \psi = 0 \tag{2.5}$$

on the black hole exterior of a subextremal ($|a| < M$) Kerr spacetime. Then the following uniform pointwise estimates hold for some $\eta \in (0, 1)$:

$$\left| \psi - \frac{Q_0(\tau + r)}{\tau^2(\tau + 2r)^2} \right| \le \frac{E_0}{(\tau + 2r)\tau^{2+\eta}}, \tag{2.6}$$

$$\left| r^{-\ell}\psi_{\ell=1} - \frac{Q_\ell(r,\theta,\phi)(\tau + r)}{\tau^3(\tau + 2r)^3} \right| \le \frac{E_0}{(\tau + 2r)^2\tau^{3+\eta}}, \tag{2.7}$$

$$\left| r^{-\ell}\psi_{\ge\ell} - \frac{Q_\ell(r,\theta,\phi)(\tau + r)}{\tau^{2+\ell}(\tau + 2r)^{2+\ell}} \right| \le \frac{E_0}{(\tau + 2r)^{1+\ell}\tau^{2+\ell+\eta}} \quad \text{when } a = 0. \tag{2.8}$$

Here τ is a coordinate corresponding to a hyperboloidal slicing of the exterior with the slices ending at the horizon and future null infinity, and Q_ℓ is a bounded function in r

tending as $r \to \infty$ to an explicitly computable initial data quantity related to the Newman–Penrose charges. Finally, $\psi_{\geq \ell}$ denotes the projection of ψ to the standard spherical harmonics defined with respect to Boyer–Lindquist (θ, ϕ) coordinates and E_0 is a constant determined from a weighted initial data Sobolev norm.

The asymptotics (2.8) were first proved for $\ell = 0$, on a class of asymptotically flat spherically symmetric spacetimes including Schwarzschild and Reissner–Nordström, by Angelopoulos–Aretakis–Gajic [8]. Their subsequent work [9] extracts also a logarithmic subleading term in the large τ expansion of the radiation field (defined as the limit $\lim_{r\to\infty} r\psi(\tau, r, \theta, \phi)$) for spherically symmetric waves. On a class of asymptotically flat spacetimes which include subextremal Kerr spacetimes, Hintz [106] gave the first proof of (2.6). The proof is based on a careful spectral analysis near zero energy, see Section 2.3.4, with direct antecedents in the work of Donninger–Schlag–Soffer [71] and Tataru [197] which proved upper bounds of $|\psi|$ consistent with (but for $\ell \geq 1$ weaker than) the asymptotics stated above. The paper [106] also proves the estimate (2.8) in spatially compact sets and identifies $r^\ell Q_\ell(r, \theta, \phi)$ as a *generalized zero mode* of the wave equation, namely the unique stationary solution of $\Box_{g_{\Lambda=0,M,a=0}}(r^\ell Q_\ell) = 0$ with the property that $r^\ell Q_\ell(r, \theta, \phi) = q_\ell(r)Y$, $q_\ell = r^\ell + \mathcal{O}(r^{\ell-1+\varepsilon})$ as $r \to \infty$, where Y is a suitable degree ℓ spherical harmonic (depending on the initial data).

Angelopoulos–Aretakis–Gajic [11, 12] gave a physical space proof of Theorem 8. This interpolates a refinement (introducing carefully constructed higher order commutators adapted to the angular modes) of the r^p-method [65], which gets one close to the optimal rates, with a clever way to exploit the conservation of the Newman–Penrose charges along null infinity. In fact, the Newman–Penrose charges in Theorem 8 are not the ones associated with ψ itself but that of a "time-inverted" ψ and generically nonvanishing, even for data of compact support. Estimates analogous to (2.7) have been derived for higher modes but take a more complicated form, which we do not present here. We merely remark that obtaining the rates for higher modes in the case $a \neq 0$ is very delicate due to the coupling of angular modes (Kerr being only axisymmetric).

In the extremal spherically symmetric case (Section 2.3.2), the asymptotics are quite different [10]. In fact, the extremality of the horizon can be seen in the expansion on null infinity giving rise to speculations about the experimental detection of extremal black holes in the universe [7].

2.3.4. $\Lambda = 0$: spectral theoretic approach

Another approach to the proof of Theorem 6(2) is based entirely on spectral theory and phase space analysis. The starting point is a foliation of the spacetime by level sets of a time function t_* which are transversal to the future event horizon and asymptote to t-level sets as $r \to \infty$. (In practice, it is more convenient to work instead with t_* whose level sets are transversal to future null infinity.) Since $|\psi| < Ce^{Ct_*}$ for some $C > 0$, one can write ψ

as the inverse Fourier transform[4]

$$\psi(t_*) = \int_{\Im\sigma = C+1} e^{-i\sigma t_*} \widehat{\Box}(\sigma)^{-1} \hat{f}(\sigma)\,\mathrm{d}\sigma, \quad \Box = \Box_{g_{M,a}}, \tag{2.9}$$

where $\hat{f}(\sigma)$ is an explicit expression involving the Cauchy data of ψ, and the *spectral family* $\widehat{\Box}(\sigma)$ is obtained from $\Box$ by replacing ∂_{t_*} by $-i\sigma$. The inverse $\widehat{\Box}(\sigma)^{-1}$ in (2.9) is the *outgoing resolvent*, with range comprised of functions which decay as $r \to \infty$. The strategy is now to shift the contour of integration down to the real axis $\Im\sigma = 0$. Executing this relies on several ingredients.

The first ingredient is the analyticity of the resolvent $\widehat{\Box}(\sigma)^{-1}$ in $\Im\sigma > 0$ as well as the existence the limiting resolvent as $\Im\sigma \searrow 0$. This is established in two steps. The first step is that for $\Im\sigma \geq 0$, one can realize $\widehat{\Box}(\sigma)$ as a Fredholm operator between suitable function spaces (based on weighted L^2-Sobolev spaces), with locally uniform estimates; we only discuss this in the case $\sigma \in \mathbb{R}$. The operator $\widehat{\Box}(\sigma)$ satisfies elliptic estimates except in the region where $\partial_{t_*} = \partial_t$ is not timelike, which happens precisely in the ergoregion and the black hole interior. But microlocally, i.e., in phase space, the flow of the Hamiltonian vector field associated to the principal symbol of $\widehat{\Box}(\sigma)$—which here means the null-geodesic flow lifted to phase space restricted to the annihilator of ∂_{t_*}, and projecting out the t_*-coordinate—has useful structure: there is a source at $N^*\{r = r_+\} \setminus o$ (the conormal bundle of the event horizon); this is related to the classical red-shift effect. There, one gets free microlocal estimates for u solving

$$\widehat{\Box}(\sigma)u = f \tag{2.10}$$

in terms of f, called *radial point estimates* **[201, §2.4]**. These take the form

$$\|Au\|_{H^s} \leq C\left(\left\|G\widehat{\Box}(\sigma)u\right\|_{H^{s-1}} + \|\chi u\|_{H^{-N}}\right)$$

where $A, G \in \Psi^0$ are pseudodifferential operators localizing to suitable conic neighborhoods of $N^*\{r = r_+\}$, and χ localizes near $r = r_+$ in the base $\mathcal{M}$. The classical Duistermaat–Hörmander theorem on the propagation of regularity **[72]** allows one to propagate this control on u along the null-geodesic flow, which in the case $a \neq 0$ enters the black hole exterior, but which in any case ultimately enters the black hole interior.

Another source of nonellipticity of $\widehat{\Box}(\sigma)$ for real $\sigma \neq 0$ is due to the presence of an asymptotically flat end of the spatial slice $t_*^{-1}(0)$, and concerns the lack of arbitrary *decay* rather than regularity; indeed one has to allow for u in (2.10) to have outgoing asymptotics $u \sim r^{-1}e^{i\sigma r}$. This can be captured microlocally in Melrose's scattering calculus **[162]** and indeed historically was the first instance of a microlocal radial point estimate.

Altogether, one obtains locally uniform estimates in the punctured upper half-plane

$$\|u\|_{H^{s,\ell}} \leq C\left(\left\|\widehat{\Box}(\sigma)u\right\|_{H^{s-1,\ell+1}} + \|u\|_{H^{-N,-N}}\right), \quad \Im\sigma \geq 0,\ \sigma \neq 0, \tag{2.11}$$

4 The choice of sign of σ in this formula (and thus also in the corresponding formula for the Fourier transform) is conventional.

where $H^{s,\ell} = r^{-\ell}H^s$ is a weighted Sobolev space. Analogous estimates on dual function spaces for the adjoint $\widehat{\Box}(\sigma)^*$ give the claimed Fredholm property of $\widehat{\Box}(\sigma)$. The invertibility of $\widehat{\Box}(\sigma)$, together with sharp mapping properties of the inverse, follows from the triviality of the kernel. This is the place, finally, where the mode stability results [193, 209] enter the analysis. Direct differentiation in σ then gives high regularity of $\widehat{\Box}(\sigma)^{-1}$ in $\sigma \neq 0$.

Uniform analysis near $\sigma = 0$ is delicate due to the degeneration of $\widehat{\Box}(\sigma)$ at spatial infinity when $\sigma \searrow 0$. Sharp Fredholm estimates were obtained by Vasy [202, 204] using a second microlocal combination of the scattering calculus (for $\sigma \neq 0$) and the b-calculus (for $\sigma = 0$) [161], following direct resolvent estimates [29] and (in a restricted geometric setting) direct constructions of the resolvent kernel [95–97, 101]. While bounds and mild (conormal) regularity of the resolvent near zero energy are sufficient to obtain some decay, Hintz [106] developed a method to obtain the first few terms of a polyhomogeneous (generalised Taylor) expansion of $\widehat{\Box}(\sigma)^{-1}\hat{f}(\sigma)$ at $\sigma = 0$. This uses resolvent identities and, in turns, the inversion of $\widehat{\Box}(0)$ and a rescaled model problem[5] capturing the transition from zero to non-zero spectral parameters. The expansion, upon restriction to bounded spatial subsets, takes the schematic form

$$\widehat{\Box}(\sigma)^{-1}\hat{f}(\sigma) = [\text{holomorphic}] + \sigma^2 \log(\sigma + i0)c + [\text{more regular error terms}] \quad (2.12)$$

for some constant $c \in \mathbb{C}$. Upon taking the inverse Fourier transform, the strongest singular term will give rise to the leading order long time asymptotics as $t_* \to \infty$, given by $2ct_*^{-3}$; the regularity of the error terms determines the decay rate of the remainder.

The second ingredient required to execute the contour shifting in the integral (2.9) concerns *high energy estimates*, i.e., quantitative bounds on $\widehat{\Box}(\sigma)^{-1}$ as $\Re\sigma \to \infty$ (locally uniformly in $\Im\sigma \geq 0$). It is in this high frequency regime that the structure of the trapping becomes relevant. To explain this in rough terms, consider the *semiclassically rescaled equation*

$$P_{h,z}u := h^2\widehat{\Box}(h^{-1}z)u = f, \quad h = |\sigma|^{-1}, \quad z = \frac{\sigma}{|\sigma|} = 1 + \mathcal{O}(h). \quad (2.13)$$

As a guiding example, consider briefly the Minkowskian wave operator $\Box = -D_{t_*}^2 + \sum D_{x^j}^2$; then $P_{h,z} = \sum(hD_{x^j})^2 - 1 + \mathcal{O}(h)$, and thus according to geometric optics, high frequency ($\sim h^{-1}$) oscillations have momenta in $\{\sum \xi_j^2 - 1 = 0\}$ and propagate along lifted geodesics, which are the projections to spatial coordinates and momenta of Minkowskian null-geodesics. Generalizing to the Kerr case, high frequency oscillations of u solving (2.13) are localized in the *characteristic set* of spatial momenta ξ so that $-\mathrm{d}t_* + \xi$ is lightlike, and propagate along projections (to the spatial phase space) of lifted null-geodesics. The dynamics of this projected lifted null-geodesic flow is more ornate than in the bounded frequency regime: there is now a trapped set (in the Schwarzschild case: the restriction of Γ in (1.15) to $t = 0$ and $\sigma = -1$ if we take $t_* = t$ near $r = 3M$) at which the flow is ν-normally hyperbolic for all ν. However, *purely based on the dynamical nature of the trapping* and its interplay with the symplectic structure of phase space, one can apply black box results [77, 210] (see

5 It is obtained by taking $\hat{r} = \sigma r$ and considering the limit $\sigma \to 0$ with fixed $\hat{r}$.

also [108]) on the propagation of semiclassical regularity (i.e., bounds on amplitudes of high frequency oscillations) for microlocal control of u there. Combining this with semiclassical radial point estimates at the event horizon [201, §2.8] [78, APPENDIX E] and at spatial infinity [203, 205], one ultimately obtains estimates in semiclassical function spaces (with each derivative weighted by a factor of h) analogous to (2.11),

$$\|u\|_{H_h^{s,\ell}} \leq C\big(h^{-1-\varepsilon}\|P_{h,z}u\|_{H_h^{s-1,\ell+1}} + h^N\|u\|_{H_h^{-N,-N}}\big),$$

where the $\varepsilon > 0$ loss can be sharpened to a logarithmic loss when $\Im z \geq 0$; this loss comes from the trapping estimate. For small $h > 0$, the second, error, term on the right can be absorbed into the left-hand side, and one obtains the invertibility (with quantitative bounds) of $P_{h,z}$ and thus of $\widehat{\Box}(\sigma)$.

Equipped with these high energy estimates, one can justify the contour shifting down to the real axis; the loss of powers of $h^{-1} = |\sigma|$ corresponds to a necessary loss [186] of regularity of the solution (when estimated in decaying function spaces) relative to the initial data.

Important precursors of the low frequency analysis of [106, 204] are the works by Donninger–Schlag–Soffer [71] (based on direct resolvent kernel constructions in spherical symmetry) and Tataru [197] on Price's law (based on resolvent estimates and weak versions of the expansion (2.12)). In Tataru's approach, uniform resolvent control down to the real axis is deduced from the assumption of a suitable form of *local energy decay*; this assumption needs to be verified separately. (Thus, [197] upgrades weak to sharp decay.) In the full subextremal range, local energy decay was first proved in the aforementioned [66], following earlier work for slow angular momenta [6, 64]. For more on the relationship between mode stability and local energy decay, see [165, 167].

2.3.5. $\Lambda > 0$: exponential decay and quasinormal mode expansions

For linear scalar waves on slowly rotating Kerr–de Sitter black hole spacetimes $(M, g_{\Lambda,M,a})$, Dyatlov [73–75] proved a full asymptotic expansion

$$\psi(t_*, x) = \sum_{\Im\sigma_j \geq -\alpha} e^{-i\sigma_j t_*} t_*^k a_{jk}(x) + \mathcal{O}(e^{-\alpha t_*}), \quad x = (r, \theta, \phi), \tag{2.14}$$

for all $\alpha \in \mathbb{R}$ avoiding the discrete set of accumulation points of $\{-\Im\sigma_j\}$. Here, the σ_j are the *resonances* or *quasinormal modes* (QNMs);[6] they are the poles of the *meromorphic* continuation of the resolvent $\widehat{\Box_{g_{\Lambda,M,a}}}(\sigma)^{-1}$ from $\Im\sigma \gg 1$ to the complex plane in σ. The structure of the set $\{\sigma_j\}$ was analyzed in great detail in [75]; here we only record that the only resonance with $\Im\sigma_j \geq 0$ is $\sigma_0 := 0$ (with multiplicity 1 and a_{00} a constant), and thus ψ decays exponentially fast to a constant. The existence of a meromorphic continuation of the resolvent (as opposed to the nonalgebraic singularity (2.12) in the case $\Lambda = 0$) is due to the presence of the cosmological horizon and the related fact that one work with a *compact* spatial manifold;

6 In the absence of multiplicities ($k = 0$), a_{j0} is a corresponding mode solution (or *resonant state*).

the general microlocal framework for the relevant spectral theory (both for bounded and high frequencies) was provided in Vasy's seminal work [201]. (The analyticity of the quasinormal mode solutions, for analytic choices of time functions t_*, was proved in [148], based on [89].)

In the Schwarzschild–de Sitter case, (2.14) was proved by Bony–Häfner [28] in the black hole exterior, with uniformity down to the horizons provided in [164] using the relationship of SdS and asymptotically hyperbolic spaces [160, 163]. For results on the set of resonances and mode solutions in the small black hole limit $M\Lambda^2 \searrow 0$, see [117]. Results on quasinormal modes on charged black hole spacetimes were proved in [22,127]. We remark that energy methods [62] have thus far been successful in proving superpolynomial decay to constants.

2.3.6. $\Lambda < 0$: stable trapping and logarithmic decay

The existence of the conformal boundary (where null geodesics are reflected) in conjunction with the existence of trapped geodesics leads to the phenomenon of *stable* trapping, which gives rise to an inverse logarithmic rate for solutions provided the Hawking–Reall bound is satisfied. (The Hawking–Reall bound ensures the existence of a globally causal Killing field on the exterior and hence eliminates the difficulty of superradiance.) This rate was established as an upper bound in [120] and is in fact optimal for general solutions, as follows either from quasimode constructions [121] or the existence of quasinormal modes exponentially close to the real axis [90,91]; see [208] for the development of a general theory of quasinormal modes in this setting. (Inverse logarithmic decay rates are familiar from the obstacle problem in Minkowski space [33].) Outside the Hawking–Reall bound, Dold [70] constructed exponentially growing solutions using techniques from [192].

Finally, the behavior is expected to be radically different if dissipative boundary conditions are imposed on the scalar field, in which case strong decay is likely to hold.

2.4. Linear stability

Here, we only discuss the case $\Lambda = 0$. The reason is that there are currently no rigorous results for $\Lambda < 0$ in the case of reflecting boundary conditions, whereas for $\Lambda > 0$ nonlinear stability was proved directly (see Section 2.5) without prior work on linear stability.

Theorem 9 ([5, 100]). *Linear stability holds for slowly rotating Kerr spacetimes.*

A natural approach to Theorem 9 is to try to reduce it to the toy problem. However, both the generalized harmonic gauge (Section 1.2) as well as the double null gauge (Section 1.3) lead to a highly coupled *system* of linearized equations. In the following, we describe several different approaches to address this problem.

2.4.1. The double null approach

The first linear stability result was proved by Dafermos–Holzegel–Rodnianski in [58] and concerns the linear stability of the Schwarzschild metric. The approach of [58] is based on expressing (1.1) in a double null gauge and linearizing the resulting system with respect to Schwarzschild. For clarity, we describe the main ideas more generally for the linearization around Kerr. Let us fix the differentiable structure of the Pretorius–Israel double null coordinates (u, v, θ) on the Kerr manifold with parameters (M, a) and consider a one-parameter family of metrics expressed in these coordinates

$$\boldsymbol{g}(\varepsilon) = -4\boldsymbol{\Omega}^2(\varepsilon)\mathrm{d}u\,\mathrm{d}v + \boldsymbol{\not g}_{AB}(\varepsilon)\big(\mathrm{d}\theta^A - \boldsymbol{b}^A(\varepsilon)\mathrm{d}v\big)\big(\mathrm{d}\theta^B - \boldsymbol{b}^B(\varepsilon)\mathrm{d}v\big) \tag{2.15}$$

such that $\varepsilon = 0$ corresponds to the Kerr metric of mass M and specific angular momentum a. In other words, we identify the ingoing and outgoing null cones of each member of the family with the respective cones of the Kerr exterior.

If $\boldsymbol{\xi}$ is an $\mathbb{S}^2_{u,v}$-tensor denoting an arbitrary Ricci coefficient or curvature component associated with $\boldsymbol{g}(\varepsilon)$ and ξ denotes the analogous component for $\boldsymbol{g}(0)$, then $\boldsymbol{\xi} - \xi$ is a map from $\mathbb{R}$ into the bundle of $\mathbb{S}^2_{u,v}$-tensors on $\mathcal{M}$ and we can hence define

$$\overset{(1)}{\xi} := \frac{\mathrm{d}}{\mathrm{d}\varepsilon}(\boldsymbol{\xi} - \xi)|_{\varepsilon=0},$$

which we call a linearized Ricci coefficient or curvature component, respectively. Note that we can indeed consider the difference of the two tensors as we have identified the notion of $\mathbb{S}^2_{u,v}$-tensors for the family (2.15), i.e., we have fixed the tensor bundle of $\mathbb{S}^2_{u,v}$-tensors on the manifold independently of ε.

To produce the linearized Bianchi and null structure equations, one writes down the null structure and Bianchi equations once for general ε (in bold font) and once for $\varepsilon = 0$ (in standard font) and then subtracts the two equations ignoring terms of order ε^2. This linearization process is entirely straightforward and particularly simple in the Schwarzschild case where all $\mathbb{S}^2_{u,v}$-one-forms and symmetric traceless tensors vanish identically for the (spherically symmetric) background. It produces a system of equations for $\mathbb{S}^2_{u,v}$-tensors representing linearized curvature components and Ricci coefficients on the Kerr manifold with all differential operators being defined with respect to the Kerr background metric. For instance, in the (algebraically simpler) Schwarzschild case $a = 0$, where the Pretorius–Israel double null coordinates become the familiar Eddington–Finkelstein double null coordinates, the linearization of (1.10), (1.11) reads

$$\Omega \not\nabla_3\big(r\Omega^2\overset{(1)}{\alpha}\big) = -2\Omega^2 r \not{\mathcal{D}}_2^\star\big(\Omega\overset{(1)}{\beta}\big) - \frac{3M}{r^2}\Omega^3\overset{(1)}{\hat\chi}, \tag{2.16}$$

$$\Omega \not\nabla_4\big(r^4\Omega^{-1}\overset{(1)}{\beta}\big) = -r^3\not{\mathrm{d}}\mathrm{iv}\big(r\overset{(1)}{\alpha}\big), \tag{2.17}$$

and the structure equation (1.8) becomes

$$\Omega \not\nabla_4\big(r^2\overset{(1)}{\hat\chi}\Omega\big) + \frac{2M}{r^2}\big(r^2\overset{(1)}{\hat\chi}\Omega\big) = -r^2\Omega^2\overset{(1)}{\alpha}. \tag{2.18}$$

We now collect an important result, which is due to Teukolsky **[200]**. For this we recall from Section 1.4.4 the algebraically special frame of Kerr $(e_3^{as}, e_4^{as}, e_1^{as}, e_2^{as})$. We define an ε-dependent family of frames $(\boldsymbol{e}_3^{as}, \boldsymbol{e}_4^{as}, \boldsymbol{e}_1^{as}, \boldsymbol{e}_2^{as})$ which is null with respect to $\boldsymbol{g}(\varepsilon)$ and reduces for $\varepsilon = 0$ to $(e_3^{as}, e_4^{as}, e_1^{as}, e_2^{as})$. We then define the linearized quantities

$$\overset{(1)}{\alpha}_{as}(e_A^{as}, e_B^{as}) := \lim_{\varepsilon\to 0}\frac{\mathbf{Riem}(\boldsymbol{e}_4^{as}, \boldsymbol{e}_A^{as}, \boldsymbol{e}_4^{as}, \boldsymbol{e}_B^{as})}{\varepsilon}, \tag{2.19}$$

$$\overset{(1)}{\underline{\alpha}}_{as}(e_A^{as}, e_B^{as}) := \lim_{\varepsilon \to 0} \frac{\mathbf{Riem}(\boldsymbol{e}_3^{as}, \boldsymbol{e}_A^{as}, \boldsymbol{e}_3^{as}, \boldsymbol{e}_B^{as})}{\varepsilon}. \tag{2.20}$$

Note that these quantities are generally *not* $\mathbb{S}^2_{u,v}$-tensors unless $a = 0$ but can be interpreted as horizontal tensors by identifying the horizontal structures (i.e., the spaces $g(\varepsilon)$-orthogonal to the distribution $(\boldsymbol{e}_3^{as}, \boldsymbol{e}_4^{as})$) for different ε just as we did for $\mathbb{S}^2_{u,v}$-tensors earlier. They can also be viewed as elements of a complex line bundle of spin-± 2-weighted functions, see **[200]** and **[57, §2.2]**. Note that for $a = 0$ we have $\overset{(1)}{\alpha}_{as}(e_A^{as}, e_B^{as}) = \overset{(1)}{\alpha}(e_A, e_B)$ and $\overset{(1)}{\underline{\alpha}}_{as}(e_A^{as}, e_B^{as}) = \overset{(1)}{\underline{\alpha}}(e_A, e_B)$ as the double null frame agrees with the algebraically special frame. Also one may check that (2.19) and (2.20) do not depend on the particular choice of frame $(\boldsymbol{e}_3^{as}, \boldsymbol{e}_4^{as}, \boldsymbol{e}_1^{as}, \boldsymbol{e}_2^{as})$ described above. In other words, there is a gauge invariance to order ε under $\boldsymbol{g}(\varepsilon)$-frame rotations.

Proposition (**[200]**). The quantities $\overset{(1)}{\alpha}_{as}$ and $\overset{(1)}{\underline{\alpha}}_{as}$ satisfy (individually) decoupled wave equations, called the spin ± 2 Teukolsky equations.

In the case $a = 0$, the Teukolsky equation takes the simple form (as easily checked from (2.16)–(2.18))

$$\Omega \nabla\!\!\!/_4 \Omega \nabla\!\!\!/_3 \big(r\Omega^2 \overset{(1)}{\alpha}\big) + \frac{2\Omega^2}{r^2} r^2 \mathcal{D}_2^\star \mathrm{d}\!\!/\mathrm{iv} \big(r\Omega^2 \overset{(1)}{\alpha}\big) + \frac{4}{r}\left(1 - \frac{3M}{r}\right) \Omega \nabla\!\!\!/_3 \big(r\Omega^2 \overset{(1)}{\alpha}\big) + \frac{6M\Omega^2}{r^3} \big(r\Omega^2 \overset{(1)}{\alpha}\big) = 0, \tag{2.21}$$

which we will focus on to convey some of the main ideas that follow. The problem with equation (2.21) is that because of the first order term, the standard physical space techniques for the toy problem do not apply: there is no natural conserved energy and the standard approach to prove (2.3) fails. Nevertheless, we have the following result:

Theorem 10. **[57,58,157]** *Solutions to the spin ± 2 Teukolsky equations arising from suitably weighted initial data on a Kerr spacetime with $|a| \ll M$ decay inverse polynomially in time on the black hole exterior.*

Proof. For $a = 0$, one may apply the physical space transformations

$$r^5 \overset{(1)}{P} = \frac{r^3}{\Omega} \nabla\!\!\!/_3 \big(\overset{(1)}{\psi} r^3 \Omega\big), \quad r^3 \Omega \overset{(1)}{\psi} = -\frac{1}{2}\frac{r^2}{\Omega} \nabla\!\!\!/_3 \big(r\Omega^2 \overset{(1)}{\alpha}\big) \tag{2.22}$$

introduced in **[58]**. These transformations are physical space versions of transformation introduced by Chandrasekhar in **[38]** at the mode-decomposed level. The point is that the quantity $\overset{(1)}{P}$ satisfies the *Regge–Wheeler* equation

$$\Omega \nabla\!\!\!/_3 \Omega \nabla\!\!\!/_4 \big(r^5 \overset{(1)}{P}\big) + \frac{2\Omega^2}{r^2} r^2 \mathcal{D}_2^\star \mathrm{d}\!\!/\mathrm{iv} \big(r^5 \overset{(1)}{P}\big) + V\big(r^5 \overset{(1)}{P}\big) = 0, \tag{2.23}$$

where V is a potential with favorable properties. Equation (2.23) turns out to be an equation for which the estimates (2.2) and (2.3) can be proven, i.e., the toy model theory applies. Once (2.3) is proven for $\overset{(1)}{P}$ one may derive from (2.22) the identity

$$\frac{1}{2}\Omega \nabla\!\!\!/_3 \big(r|r^3\Omega \overset{(1)}{\psi}|^2\big) + \frac{1}{2}\Omega^2 |r^3 \Omega \overset{(1)}{\psi}|^2 = r^4 \overset{(1)}{P} \Omega^2 \cdot \overset{(1)}{\psi} r^3 \Omega. \tag{2.24}$$

Applying Cauchy–Schwarz inequality on the right and using the integrated decay estimate for $\overset{(1)}{P}$, this can be integrated forwards to produce boundedness and integrated decay estimates for $\overset{(1)}{\psi}$. Repeating the same procedure for the pair $(\overset{(1)}{\psi}, \overset{(1)}{\alpha})$, one obtains the desired estimates for $\overset{(1)}{\alpha}$. Obviously, this process loses derivatives but these can be recovered by studying the wave equations for $\overset{(1)}{\psi}$ and $\overset{(1)}{\alpha}$ with the just obtained a priori estimates on the lower order terms.

For $|a| \ll M$, a straightforward modification of the transformations (2.22) produces an analogue of (2.23), which is now a coupled wave equation schematically of the form

$$\Box_{RW,g_{M,a}} \overset{(1)}{P} = a\mathcal{F}\big(\overset{(1)}{\psi}, \overset{(1)}{\alpha}\big) \tag{2.25}$$

where $\Box_{RW,g_{M,a}}$ is the Regge–Wheeler operator associated with the Kerr metric $g_{M,a}$ to which again the techniques from the toy problem apply and $\mathcal{F}(\overset{(1)}{\psi}, \overset{(1)}{\alpha})$ denotes an explicit expression involving up to first derivatives of $\overset{(1)}{\psi}$ and $\overset{(1)}{\alpha}$. However, just as for the toy problem, proving estimates for $\Box_{RW,g_{M,a}}$ now requires frequency decomposition and a form of separability of the equations, which makes the problem technically more involved. Moreover, the transport estimates for the lower order quantities are now directly coupled to (2.25) so all estimates have to be proven at the same time. Key are the smallness of $|a|$ in the coupling as well as a special structure in the right-hand side of (2.25), which needs to be identified and exploited. ■

In the full subextremal case $|a| < M$, we have the following recent milestone:

Theorem 11 ([194]). *Theorem 10 holds for the full subextremal range $|a| < M$ provided solutions are a priori assumed to be future-integrable.*

We remark that the assumption of future-integrability in Theorem 11 ensures that one can take the Fourier transform in time and hence prove estimates at the level of the radial ODE governing the dynamics of the frequency decomposed pieces of the solution. For the wave equation, proving these estimates (i.e., Theorem 11) is the main difficulty in the proof of Theorem 6. Removing the assumption of future integrability is expected to follow along the lines of [66] and would lead to a proof of Theorem 10 for the full subextremal range and complete our picture of the dynamics of the Teukolsky equation.

The proof of Theorem 11 adds several new ideas to the proof of Theorem 10. It requires a much more subtle construction of the multipliers and various applications of the Teukolsky–Starobinski identities since smallness of $|a|$ cannot be exploited. We finally note also the papers [80, 81] for related results on the Teukolsky equation.

We pause for a moment to recap what we have achieved in proving Theorem 9. We have obtained a linearized system of equations in double null gauge and we have shown that certain quantities within this system satisfy decay estimates. In the $a = 0$ case, these are precisely $\overset{(1)}{\alpha}$ and $\overset{(1)}{\underline{\alpha}}$. The second and equally important step is to identify a hierarchical structure in the linearized system that allows proving boundedness and decay for all dynamical quantities, preferably without loss of derivatives (the latter with the nonlinear problem in mind) from the quantities that have been shown to decay. This was achieved for $a=0$ in [58]. This part of the proof relies on a complete understanding of two important classes of special solutions, which we again discuss in the $a=0$ case:

(A) An explicit 4-dimensional family of solutions to the system arising from the fact that the Schwarzschild solution sits as a one-parameter family inside the Kerr family. Since to specify a nearby Kerr from the point of view of Schwarzschild metric one needs to prescribe both a direction of rotation (i.e., a 3-vector) and a change of mass (a scalar), the corresponding family is indeed 4-dimensional.

(B) An infinite-dimensional family of pure gauge solutions, parametrized by a set of spacetime functions $f_i(u,v,\theta)$. These arise from the fact that certain infinitesimal coordinate transformations preserve the double null form (2.15) to order ε^2 while changing the dynamical quantities to order ε in an explicit fashion. For instance, the coordinate transformation

$$\tilde{u}=u, \quad \tilde{v}=v+\varepsilon f_2(v,\theta), \quad \tilde{\theta}^A=\theta^A+\varepsilon\frac{2}{r(u,v)}\not{g}^{AB}\partial_A f_2(v,\theta)$$

is easily seen to preserve the double null form (2.15) to order ε. These transformations are the infinitesimal versions of a change of double null foliation, i.e., perturbing the spheres and the foliations of the cones slightly. At the linearized level they generate a special class of solutions which are called pure gauge solutions. These solutions may be added to a given reference solution of the linearized system to achieve a specific normalization of the linearized Ricci coefficients on suitable chosen cones of the background. Finally, one observes that pure gauge solutions always have $\overset{(1)}{\alpha}=0=\overset{(1)}{\underline{\alpha}}$, i.e., the Teukolsky quantities are gauge invariant.

With these observations, we can state the following slightly more specific version of Theorem 9 for $a=0$.

Theorem 12 ([58]). *All solutions to the linearized vacuum Einstein equations around Schwarzschild arising from regular asymptotically flat initial data*

- *remain uniformly bounded on the exterior and*
- *decay inverse polynomially (through a suitable foliation) to a standard linearized Kerr solution (a 4-dimensional space) after adding a pure gauge solution which can itself be estimated by the size of the data.*

The point here is that in a gauge that is normalized with respect to the cones where the initial data is prescribed ("initial data gauge") one will only be able to prove *boundedness*. In order to see *decay*, one needs to add a pure gauge solution that achieves $\Omega^{-1}\overset{(1)}{\Omega}=0$ on $\mathcal{H}^+$ for the sum of the two solutions, i.e., one needs to normalize the solution with respect to the future event horizon to see decay. This is the future gauge or teleological normalization. While the pure gauge solution required to do this has to be determined dynamically by solving an ODE along the event horizon, it can still be bounded uniformly by initial data.

The reason that going to the teleological normalization is required to prove decay can be understood from the fact that while the (linearized) Bianchi equations capture the hyperbolic nature of the Einstein equations, the (linearized) null structure equations also involve *transport* equations. Solutions to transport equations do generally not decay to zero if integrated from initial data. On the other hand, integrating them backwards from the future (in this case, the event horizon) with zero data captures the decay (provided the right-hand side of the relevant transport equation has been shown to decay sufficiently fast, which is, for instance, the case if it involves a Teukolsky quantity). Geometrically, one may say that in the initial data normalized gauge the solution converges to a linearized Kerr but not in the standard double null coordinates.

We note that while we have described parts of the argument for the case $a = 0$ (which is the one treated in [58]), the double null approach can be pursued also in the case $|a| \ll M$ by treating the errors arising from non-vanishing a in the transport equation perturbatively and using Theorem 10. This is a problem that is likely to be solved in the near future and would provide a complete proof of Theorem 9 in double null gauge. Finally, generalizing carefully the transformations (2.22), linear stability of the Reissner–Nordström solution to the coupled Einstein–Maxwell system has been proven in [92].

2.4.2. Generalized harmonic gauge

Häfner–Hintz–Vasy [100] proved the linear stability of slowly rotating Kerr black holes for initial data with standard decay bounds on the initial data (roughly pointwise $o(r^{-1})$ and $o(r^{-2})$). Their proof is based on a precise analysis of the resolvent of a linearized gauge-fixed Einstein operator. More precisely, when studying the linear stability of $g_{M,a}$, $|a| \ll M$, [100] uses the linearization of the generalized harmonic gauge 1-form

$$W_\mu = g_{\mu\nu} g^{\kappa\lambda}\big(\Gamma(g)^\nu_{\kappa\lambda} - \Gamma(g_{M,a})^\nu_{\kappa\lambda}\big)$$

around $g = g_{M,a}$, which maps $h \mapsto \operatorname{div}_g \mathsf{G}_g h$. One then considers the linearization L of the quasilinear wave operator

$$P(g) := \operatorname{Ric}(g) - (\delta_g^* + q)W$$

around $g = g_{M,a}$. Here q is a suitable stationary bundle map (i.e., differential operator of order 0) from 1-forms to symmetric 2-tensors, used to implement *constraint damping* below. This linearization maps

$$L : h \mapsto D_g \operatorname{Ric}(h) - (\delta_g^* + q) \operatorname{div}_g \mathsf{G}_g h.$$

The principal part of L is $-\frac{1}{2}\Box_g$, and thus the Fredholm theory for the spectral analysis for the scalar wave operator sketched in Section 2.3.4 is available for the analysis of $\hat{L}(\sigma)$, $\Im\sigma \geq 0$, as well. High energy estimates require the verification of a sign condition on the subprincipal symbol at trapped set (required for application of the black box high energy estimates [77]), which was first verified in [104], and which can be shown to amount to polynomial bounds for the length of vectors that are parallel transported along trapped null-geodesics (the latter was proved in the general Kerr case in [159]).

Existence of the resolvent $\hat{L}(\sigma)^{-1}$ for nonzero σ then reduces to the problem of proving mode stability for metric perturbations; moreover, the behavior near $\sigma = 0$ is complicated due to the presence of stationary solutions (linearized Kerr metrics in a suitable gauge). Furthermore, it is (for robustness under perturbations, and also for eventual nonlinear purposes) important to *not* require the metric perturbations h to satisfy the linearized constraint equations at the Cauchy hypersurface $t_* = 0$. The analysis of $\hat{L}(\sigma)h = 0$ (i.e., L acting on the metric perturbation $e^{-i\sigma t_*}h$, with h outgoing) then starts off with the (linearized) second Bianchi identity, which gives the decoupled equation

$$\mathrm{div}_g\, \mathsf{G}_g(\delta_g^* + q)\eta = 0, \quad \eta = \mathrm{div}_g\, \mathsf{G}_g(e^{-i\sigma t_*}h).$$

This is a wave equation for the 1-form η, and for $q = 0$ it is indeed the tensor wave operator on 1-forms. The latter satisfies mode stability by direct calculation similarly to [114], except for the presence of a 0-mode corresponding to the Coulomb solution. The purpose of the stationary map q is to perturb this stationary solution away, thus giving mode stability for $\mathrm{div}_g\, \mathsf{G}_g(\delta_g^* + q)$ in the full closed upper half plane.[7] Thus, any mode solution h of $\hat{L}(\sigma)$ with $\Im\sigma \geq 0$ *automatically* verifies the linearized gauge condition

$$\eta = \mathrm{div}_g\, \mathsf{G}_g(e^{-i\sigma t_*}h) = 0. \tag{2.26}$$

Therefore, we also have a solution of the linearized Einstein equation *without gauge condition*,

$$D_g\mathrm{Ric}(e^{-i\sigma t_*}h) = 0. \tag{2.27}$$

Mode stability for this equation is well-known in the Schwarzschild case $(M, a) = (M_0, 0)$ [141,166,177,206,211], and [100] proceeds perturbatively off this case. Concretely, for nonzero σ, metric mode stability is the statement that $e^{-i\sigma t_*}h = \delta_g^*(e^{-i\sigma t_*}\omega)$ is a symmetric gradient (i.e., a Lie derivative when using vectors instead of 1-forms). Plugging this into the gauge condition (2.26) gives another wave equation for the gauge potential ω itself,

$$\mathrm{div}_g\, \mathsf{G}_g\delta_g^*(e^{-i\sigma t_*}\omega) = 0. \tag{2.28}$$

Mode stability for this equation implies that $\omega = 0$ and hence $h = 0$. This proves mode stability for L in the punctured upper half-plane.

For stationary perturbations ($\sigma = 0$), the mode stability for (2.27) in the Schwarzschild case implies that h is the sum of a linearized Kerr metric and a pure gauge term (i.e., a symmetric gradient). The gauge condition (2.28) then further restricts the pure gauge term $\delta_g^*\omega$ to a finite-dimensional space. Particular instances of such pure gauge terms, constructed

7 In fact, one can then show that solutions of $\mathrm{div}_g\, \mathsf{G}_g(\delta_g^* + q)\eta = 0$ with sufficiently smooth and decaying initial data decay in time to 0. Therefore, initial violations of the linearized gauge condition $\eta = 0$ decay in time; equivalently, initial violations of the linearized constraint equations for h decay in time. Hence, the addition of q implements *constraint damping*, the roots of which go back to the numerics literature [31,98].

in [100, §7], are symmetric gradients of asymptotic (as $r \to \infty$) translations $\omega = \mathrm{d}x^i + o(1)$ (note that $\mathrm{d}x^i$ is a Killing 1-form for the Minkowski metric) and asymptotic rotations. There are also generalized zero modes which are first-order polynomials in time, arising from gauge potentials ω which are asymptotic Lorentz boosts.

We stress that it is *only* at this point—i.e., where one needs to know the structure (pure gauge, or linearized Kerr) of mode solutions of the linearized Einstein vacuum equation for individual values of $\sigma \in \mathbb{C}$—that the highly delicate reductions of the linearized Einstein equations to scalar "master equations" are used (here the Regge–Wheeler [177] and Zerilli [211] equations). The a priori information, obtained by microlocal means which only rely on *qualitative* features of the null-geodesic flow, of uniform Fredholm properties of $\hat{L}(\sigma)$ acting between suitable function spaces is then easily upgraded to invertibility, regularity in σ, and the precise structure at $\sigma = 0$.

Altogether, one can then show that in the Schwarzschild case $\hat{L}(\sigma)^{-1}$ has a second-order pole at $\sigma = 0$ with explicit singular terms, plus a Hölder-regular remainder. This structure persists in the slowly rotating Kerr case, essentially since one can construct a space of generalized zero modes for small $|a|$ of the same dimension as for $a = 0$. (We remark that this construction requires, besides knowledge of the Kerr family of solutions, only soft perturbative arguments, and does not involve the Teukolsky equation.) Altogether, we have

Theorem 13 ([100]). *Let t_* be a time function with level sets transversal to the future event horizon and equal to the level sets of the Boyer–Lindquist time function t for large r. Consider a neighborhood $\mathcal{M} = [0,\infty)_{t_*} \times \Sigma$, $\Sigma = [2M_0 - \varepsilon, \infty) \times \mathbb{S}^2$, of the domain of outer communications of the mass M_0 Schwarzschild black hole restricted to the causal future of the Cauchy surface $t_* = 0$. Let $\alpha \in (0,1)$, and let $h_0, h_1 \in \mathcal{C}^\infty(\Sigma; S^2T^*_\Sigma\mathcal{M})$ be Cauchy data with*

$$|h_0| \lesssim r^{-1-\alpha}, \quad |h_1| \lesssim r^{-2-\alpha},$$

and similar bounds for 8 derivatives along $r\partial_r$ and spherical vector fields. For (M,a) close to $(M_0,0)$, let h denote the solution of the initial value problem

$$L_{M,a}h = 0, \quad (h, \mathcal{L}_{\partial_{t_*}}h)|_{t_*=0} = (h_0, h_1).$$

Then there exist (M',a'), and a vector field V lying in a 7-dimensional space $\mathcal{V}_{M,a}$ of vector fields on $\mathcal{M}$ so that

$$h = \frac{\mathrm{d}}{\mathrm{d}s} g_{M+sM',a+sa'}|_{s=0} + \mathcal{L}_V g_{M,a} + \tilde{h},$$

where $|\tilde{h}| \lesssim t_*^{-1-\alpha}$ in spatially compact regions. The space $\mathcal{V}_{M,a}$ is spanned by asymptotic translations and boosts, and an additional explicit vector field. (The latter vector field can be eliminated by a small change of the gauge condition. Asymptotic rotations are the same as infinitesimal changes of the black hole rotation axis.)

If the data (h_0, h_1) arise from initial data for the linearized Einstein equations (i.e., satisfying the linearized constraint equations), this implies the linear stability of slowly rotating Kerr black holes. However, Theorem 13 is significantly more general, as it applies to *general* data (h_0, h_1); this type of generality was crucial in the non-linear stability proof of Kerr–de Sitter black holes, see Section 2.5.2.

Note that, unlike in the double null gauge, the linearized metric h typically grows linearly in time due to the existence of asymptotic Lorentz boosts in the space $\mathcal{V}_{M,a}$. Decay to a linearized Kerr metric can only be seen after subtracting a suitable element of the 7-dimensional space $\mathcal{L}_V g_{M,a}$, $V \in \mathcal{V}_{M,a}$, of pure gauge solutions.

There have also been a number of works which employ vector field methods to prove the linear stability of the Schwarzschild metric in generalised harmonic gauges (for initial data satisfying the linearized constraints), see [124–126, 131].

2.4.3. Other approaches: outgoing radiation gauge

Andersson–Bäckdahl–Blue–Ma [5] gave the first proof of linear stability, assuming strong decay on the initial data. Their strategy is to assume suitable decay for solutions $\overset{(1)}{\alpha}_{as}$, $\overset{(1)}{\underline{\alpha}}_{as}$ (called $\psi_{\pm 2}$ in [5] in accord with classical Newman–Penrose notation) of the Teukolsky equations and recover the full metric perturbation via successive integrations in a suitable hierarchy. In order to accomplish this, [5] employs the *outgoing radiation gauge*.[8] Decay for the metric perturbation is proved via weighted Hardy inequalities. Special care has to be taken near null infinity, where the Teukolsky–Starobinsky identities (fourth-order differential identities relating ψ_{+2} and ψ_{-2}) play a key role for ensuring integrability at various stages in the hierarchy. In order to obtain decay for the metric coefficients, the initial data for the metric perturbation are required to have strong decay (roughly pointwise $o(r^{-7/2})$ and $o(r^{-9/2})$ decay for the linearized metric and second fundamental form). This in particular forces the linearized mass and angular momentum of the final linearized Kerr solution to *vanish* [2], and hence a key feature of the (nonlinear) stability problem is suppressed.

Given that decay results [57, 157] for the Teukolsky equation on slowly rotating Kerr backgrounds are known (cf. Theorem 10 above), [5] gives an unconditional proof of the linear stability (for strongly decaying data) in this regime.

2.5. Nonlinear stability

The first nonlinear stability result for any family of black hole spacetimes without symmetry assumptions was proved for slowly rotating Kerr–de Sitter black holes ($\Lambda > 0$) by Hintz–Vasy [115]. The results in the asymptotically flat Kerr setting are not quite yet complete, though stability under special symmetries [139] as well as the full codimensional stability of the Schwarzschild family [59] are known. See also [137, 138, 140] for progress in the slowly rotating case. Finally, we refer the readers to [59, §IV.2] for a discussion of (necessarily codimension restricted) nonlinear stability statements that one could attempt to prove in the *extremal* case.

8 The metric perturbation is trace-free (with respect to the background Kerr metric) and has vanishing contraction with the ingoing principal null vector field.

2.5.1. The case $\Lambda = 0$

With the linear problem resolved, the road is open to address the non-linear problem, that is to prove that *the subextremal Kerr family is nonlinearly stable*. Note that perturbations of Schwarzschild initial data are generally expected to converge to a Kerr solution with small angular momentum, so stability of the Schwarzschild family cannot hold without further restrictions on the data. However, we have the following result, which proves the nonlinear stability of Schwarzschild for the subset of data for which it actually holds:

Theorem 14 ([59]). *Nonlinear stability holds for the Schwarzschild spacetime provided the initial data lie on a codimension 3 submanifold of the moduli space of initial data.*

We emphasize again that the codimension 3 assumption is necessary because the Schwarzschild family is contained as the $a = 0$ subcase of the Kerr family. Outside the codimension 3 submanifold, one expects solutions to necessarily asymptote to a Kerr solution with $a \neq 0$, since the dimension of linearized Kerr solutions fixing the mass is equal to 3 in our parametrization. It is in this sense that Theorem 14 encompasses all data near Schwarzschild that converge back to a member of the Schwarzschild family. We note that Theorem 14 had been proved previously for polarized axisymmetric initial data in [139]. That work already contains some of the difficulties of the full problem. See also [140] for further discussion of their approach to the problem.

While capturing many of the nonlinear difficulties such as identifying the mass of the final solution, constructing teleological gauges and identifying a version of the null condition in them, the fact that the final state in Theorem 14 is Schwarzschild simplifies considerably both the algebra and the analysis. In particular, Theorem 14 can be (and is) proven using entirely physical space based techniques.

Before we provide a brief overview of the main ideas in the proof, we recall items (i)–(iii) from the characterization of nonlinear stability in Section 2.2. We remark that in the proof of Theorem 14, the global closeness of statement (ii) can be expressed at the top order energy level with respect to the same quantity that measures a suitable "initial" energy quantity, i.e., without loss of derivatives. In this sense, Theorem 14 contains a true orbital stability statement. Note also that Theorem 14 is indeed the nonlinear analogue of Theorem 12 as the latter can be viewed as the statement of linear asymptotic stability of Schwarzschild up to a three-dimensional space of initial data, which, in the linear problem, can be directly identified at the level of initial data.

Theorem 14 is proven by expressing the equations in a double null gauge and hence the natural setup is to prescribe characteristic initial data intersecting in a topological 2-sphere. There is a well-established procedure, indicated at the end of Section 1.3, to prescribe initial data in this setting. We now decompose the space of initial data into disjoint 3-parameter families $D = D_0 + \sum_{m=-1}^{1} \lambda_m D_m^{\mathrm{Kerr}}$, where D_0 varies over a suitable space and is of size ε_0. Here D_m^{Kerr} essentially prescribes the three $\ell = 1$ modes of the torsion on the sphere of intersection and the vector $(\lambda_{-1}, \lambda_0, \lambda_1)$ is a measure of the size of the angular momentum of the data. We prove that given any $d \in D_0$ we can find a $(\lambda_{-1}^\star, \lambda_0^\star, \lambda_1^\star)$ such that the corresponding data set D converges to Schwarzschild. We emphasize that the vector $(\lambda^\star_{-1}, \lambda^\star_0, \lambda^\star_1)$ (as well as the final mass of the solution) has to be determined teleologically, i.e., from the entire dynamics of the solution.

We now come to the main ideas of the proof. One crucial ingredient, which we already saw in the linear problem, is the use of a double null gauge which is normalized from the future, i.e., certain Ricci coefficients have to take their Schwarzschild (with mass to be determined!) values on the asymptotic hypersurfaces. The construction of such future gauges, which geometrically corresponds to finding a nearby sphere and foliating the ingoing and outgoing light cones in a prescribed fashion, is based on a implicit function theorem type argument. This uses that in the linear case we can prescribe the desired values by adding a pure gauge solution. However, the nonlinear argument is considerably complicated by the fact that the $\ell = 0$ and $\ell = 1$ modes (mass and angular momentum) require special treatment and couple nonlinearly into the iteration.

Having proven the existence of the future gauges, we can consider a solution in the initial data gauge with coordinates $(u^{\text{data}}, v^{\text{data}}, \theta^{\text{data}})$ or in the future gauge with coordinates $(u^{\text{fut}}, v^{\text{fut}}, \theta^{\text{fut}})$ with relations of the form $u^{\text{fut}} = u^{\text{data}} + f_1(u^{\text{data}}, v^{\text{data}}, \theta^{\text{data}})$, etc., in the region where both gauges are defined. As in the linear problem, we can estimate the f's provided estimates on the Ricci and curvature components are available in both of the gauges.

The proof proceeds by a large scale bootstrap argument along the following lines. Given our 3-parameter family, we consider the largest $u_f > 0$ such that in the future gauge normalized at the sphere $\mathbb{S}^2_{u_f, v_\infty}$ the following bootstrap assumptions hold in the corresponding bootstrap region $\mathcal{M}'(u_f)$ indicated in the picture below:

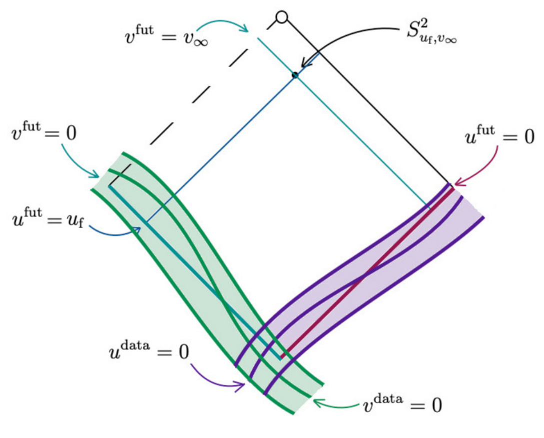

(I) We have $|f_i| \leq \varepsilon$ in the shaded ("near initial data") region of u-width ≈ 1. In particular, the $u^{\text{fut}} = 0$ cone is ε-close to the cone $u^{\text{data}} = 0$.

(II) We have decay estimates for Ricci coefficients and null curvature components minus their Schwarzschild value (which is determined from the spherical average of the curvature component ρ on $\mathbb{S}^2_{u_f,v_\infty}$) *in the future gauge*, for instance,

$$\left|r^2\left(\Omega \operatorname{tr}\chi - r^{-1}\left(1 - \frac{2M(u_f)}{r}\right)\right)\right| \leq \frac{\varepsilon}{u}, \quad \left|r^4\alpha\right| \leq \frac{\varepsilon}{u}, \quad \text{etc.}, \tag{2.29}$$

as well as a hierarchy of higher order estimates (in L^2 on spheres, null-cones and spacetime regions) for all $\vec{\lambda} \in \mathcal{R}(u_f)$ such that $|(r^5 \operatorname{c\!\!/url} \beta)_{\ell=1}(u_f, v_\infty)| \leq \frac{\varepsilon}{u_f}$ with equality on $\partial\mathcal{R}(u_f)$. (That is, for every u_f we define a corresponding set $\mathcal{R}(u_f)$ of admissible $\vec{\lambda}$ which satisfy this.)

The main task then is to show that $u_f = \infty$ by improving the above bootstrap assumptions. This proceeds along the following lines:

(1) One shows that in the shaded region the curvature components $\alpha, \underline{\alpha}$ defined with respect to the future double null gauge agree with the components defined in the initial data double null gauge up to quadratic error terms. This is a manifestation of the fact that α is gauge invariant in linear theory, that is, comparing the α's in the two gauges only produces terms quadratic in f which by bootstrap assumption (I) are indeed $O(\varepsilon^2)$.

(2) One estimates α and $\underline{\alpha}$ in the future gauge from their (now nonlinear) Teukolsky equations. The initial data are $\varepsilon_0 + O(\varepsilon^2)$ by the previous step, with ε_0 denoting the size of the initial data. Here the main challenge beyond linear theory is to estimate the nonlinear error terms, which can be shown to exhibit a version of the null condition. This improves the bounds on α and $\underline{\alpha}$ from $\frac{\varepsilon}{u}$ to $\frac{\varepsilon_0+\varepsilon^2}{u}$.

(3) One estimates all Ricci and curvature coefficients in the future gauge from the improved bounds on α and $\underline{\alpha}$ and the gauge conditions on the asymptotic hypersurfaces. This improves all estimates from $\frac{\varepsilon}{u}$ to $\frac{\varepsilon_0+\varepsilon^2}{u}$. This step involves a number of technical difficulties most of which are, however, present (in a milder form) in the linear theory.

(4) One improves $|f| \leq \varepsilon$ from the fact that by the previous step one now has, in the initial data region, bounds on the Ricci coefficients in the future gauge ($\leq \varepsilon_0 + \varepsilon^2$) and bounds on these coefficients in the initial data gauge (by Cauchy stability). Since f can be estimated from these, we deduce $|f| \leq \varepsilon_0 + \varepsilon^2$. This improves (II). Note that the fact that the initial data remains close to the old initial data is a nonlinear version of the fact that the pure gauge solution one needed to add in Theorem 12 was uniformly bounded by initial data.

(5) Having improved all the estimates, we can extend the spacetime slightly to retarded time $u_f + \delta$ and construct a new future gauge from a new future sphere. The key now is to show that $\mathcal{R}(u_f + \delta) \subsetneq \mathcal{R}(u_f)$, i.e., that the set of admissible λ of our three parameter family shrinks. This strict monotonicity can be established by carefully examining the evolution of angular momentum between the

"old" sphere and the "new" sphere. Finally, it is the topological degree of the map from the space of λ's (i.e., $\mathcal{R}(u_f)$) to the space of angular momenta in the future that is bootstrapped and ensures that for every u_f the set $\mathcal{R}(u_f)$ contains a tuple $(\lambda_{-1}, \lambda_0, \lambda_1)$ that gets mapped to zero angular momentum. This in turn implies that we can construct a sequence $(u_f)_i \to \infty$ with corresponding $\lambda_i \to \lambda^\star \in \bigcap \mathcal{R}((u_f)_i)$.

2.5.2. The case $\Lambda > 0$

The proof of the nonlinear stability of slowly rotating Kerr–de Sitter (KdS) black holes by Hintz–Vasy [115] applies spectral theoretic and microlocal methods to the analysis of a variant of the quasilinear wave equation (1.5). Consider a neighborhood

$$\mathcal{M} := [0,\infty)_{t_*} \times \Sigma, \quad \Sigma = [r_1, r_2] \times \mathbb{S}^2 \quad (r_1 = r_- - \varepsilon,\ r_2 = r_+ + \varepsilon)$$

of the black hole exterior for a subextremal Schwarzschild–de Sitter metric $g_{\Lambda,M_0,0}$ in the causal future of a spacelike hypersurface $t_*^{-1}(0) \cong \Sigma$; here, r_1, r_2 are the radii of the event and cosmological horizon, respectively, and t_* is a time function whose level sets are transversal to the future event and cosmological horizons. (See also Figure 9.) For (M, a) near (M_0, a), one can consider the KdS metric $g_{\Lambda,M,a}$ as a stationary metric on $\mathcal{M}$ with smooth dependence on (M, a); in particular, future affine complete pieces of the event and cosmological horizons of these nearby KdS black holes are contained in $\mathcal{M}$ still.

The desired asymptotic stability statement suggests writing the spacetime metric g as $g = g_{\Lambda,M,a} + \tilde{g}$ and regarding the final black hole parameters (M, a) as unknowns; the gravitational wave tail $\tilde{g}$ is an unknown as well and required to be exponentially decaying. The starting point for the gauge is the generalized harmonic gauge 1-form with coefficients $W(g)_\mu = g_{\mu\nu} g^{\kappa\lambda}(\Gamma(g)^\nu_{\kappa\lambda} - \Gamma(g^0)^\nu_{\kappa\lambda})$ measuring the failure of $(\mathcal{M}, g) \to (\mathcal{M}, g^0)$ to be a wave map; here we take

$$g^0 = g_{\Lambda,M_0,0}.$$

Since a KdS metric $g_{\Lambda,M,a}$ for $(M, a) \neq (M_0, 0)$ has no reason to satisfy the gauge condition $W(g_{\Lambda,M,a}) = 0$, one should really use the gauge condition $W(g) - W(g'_{\Lambda,M,a}) = 0$ depending on the unknown final parameters (M, a); here

$$g'_{\Lambda,M,a} = \chi g_{\Lambda,M_0,0} + (1-\chi) g_{\Lambda,M,a}$$

interpolates between $g_{\Lambda,M_0,0}$ for $t_* \leq 1$ and $g_{\Lambda,M,a}$ for $t_* \geq 2$. For further flexibility, one allows for a gauge source 1-form ϑ with compact support (or appropriate decay) in time; ϑ will lie in a suitable finite-dimensional space of 1-forms.

The nonlinear equation solved in [115] is then

$$\begin{aligned} P(M, a, \tilde{g}, \vartheta) &:= \mathrm{Ric}(g) - \Lambda g - (\delta^*_{g^0} + q)\big(W(g) - W(g'_{\Lambda,M,a}) - \vartheta\big) = 0, \\ g &= g'_{\Lambda,M,a} + \tilde{g}. \end{aligned} \tag{2.30}$$

Here, the stationary bundle map q is chosen so as to implement constraint damping, i.e., so that homogeneous solutions of the wave operator $\mathrm{div}_{g^0} \mathsf{G}_{g^0}(\delta^*_{g^0} + q)$ decay exponentially in time (i.e., it satisfies mode stability in an upper half plane $\Im\sigma \geq -\alpha$ for some $\alpha > 0$). Considerable effort is required to show the existence of such a q; see **[115, §8]**, where q is defined using a large parameter, and the required mode stability is proved using asymptotic analysis in the large parameter.

In order to analyze (2.30), consider first the linearization of the right-hand side of (2.30) in g around $g = g^0 = g_{\Lambda,M_0,0}$: it maps

$$L : h \mapsto D_{g^0}\mathrm{Ric}(h) - \Lambda h - (\delta^*_{g^0} + q)\,\mathrm{div}_{g^0}\,\mathsf{G}_{g^0}.$$

The spectral and mode analysis of this equation is in parts very close to that in the Kerr case discussed previously, namely one combines constraint damping with the metric mode stability for linearized perturbations of the Schwarzschild–de Sitter metric **[141]**. Unlike in the Kerr case, however, mode stability for the 1-form wave equation

$$\mathrm{div}_{g^0}\,\mathsf{G}_{g^0}(\delta^*_{g^0}\omega) = 0 \tag{2.31}$$

(governing those gauge potentials ω whose symmetric gradients satisfy the linearized gauge condition) is not known, and indeed can be shown to *fail* in the de Sitter case (i.e., without the presence of a black hole) due to the presence of a finite number of resonances in the upper half-plane.[9]

Thus, solutions of $Lh = 0$ have a partial resonance expansion (ignoring multiplicities) of the schematic form

$$h(t_*, x) = \left(\frac{\mathrm{d}}{\mathrm{d}s} g_{\Lambda,M_0+sM',sa'}|_{s=0} + [\text{gauge correction}]\right) + \sum_{j=1}^{N} c_j\,\delta^*_{g^0}(e^{-i\sigma_j t_*}\omega_j)$$
$$+ \mathcal{O}(e^{-\alpha t_*}),$$

where the σ_j are the finitely many modes with $\Im\sigma_j \geq 0$ corresponding to the resonances of the wave operator in (2.31); the ω_j are the corresponding mode solutions, and the c_j are suitable complex scalars depending on the initial conditions of h. The terms are then handled as follows:

(1) The gauge correction is a pure gauge term ensuring that the first summand on the right satisfies the linearized gauge condition $D_{g^0}W = 0$; it would be absent if we had $W(g_{\Lambda,M,a}) = 0$ for all (M, a) near $(M_0, 0)$. Changing the final black hole parameters from $(M_0, 0)$ to $(M_0 + M', a')$, and correspondingly changing the final gauge condition in (2.30) gives rise to essentially the same term.

(2) The nondecaying pure gauge contributions from the terms $\delta^*_{g^0}(e^{-i\sigma_j t_*}\omega_j)$ can be eliminated for late times t_* by an (explicit) change of the gauge condition, i.e., by solving

$$Lh - (\delta^*_{g^0} + q)\vartheta = 0$$

9 This is another reason why the choice of q in (2.30) requires large parameter techniques: q *cannot* be small if it is to shift these resonances all the way into the lower half-plane.

with a suitable (explicit, depending on the c_j and ω_j) gauge source 1-form ϑ; there is one such 1-form for each of the N pure gauge mode solutions.

(3) The $\mathcal{O}(e^{-\alpha t_*})$ tail contributes to the exponentially decaying tail $\tilde{g}$.

This can be rephrased as follows: the linearization of $P(M, a, \tilde{g}, \vartheta)$ at $(M_0, 0, 0, 0)$ in the argument $\tilde{g}$ is surjective if one supplements the range by a finite-dimensional space consisting of

(1) linearized black hole parameter (and associated gauge) changes—i.e., the range of the linearization of P in (M, a); and

(2) gauge modifications—i.e., the range of the linearization of P in ϑ acting on an N-dimensional space of 1-forms ϑ.

Perturbative arguments prove this surjectivity for $(M, a, \tilde{g}, \vartheta)$ near $(M_0, 0, 0, 0)$. Thus, small data initial value problems for $P(M, a, \tilde{g}, \vartheta) = 0$ can be solved using a Newton iteration scheme; due to a loss of derivatives due to trapping, **[115]** really uses a Nash–Moser iteration in the simple form given by Saint-Raymond **[185]**. Once one has a solution of the Cauchy problem for $P(M, a, \tilde{g}, \vartheta) = 0$, the standard arguments sketched in Section 1.2 imply that $g = g'_{\Lambda,M,a} + \tilde{g}$ is a solution of the initial value problem for $\mathrm{Ric}(g) - \Lambda g = 0$.

Theorem 15 (**[115]**). *Let $\Lambda > 0$ and $M_i > 0$, $a_i \in \mathbb{R}$, $|a_i| \ll M_i$. Let t_* (given by $t_* = t - F(r)$ in Boyer–Lindquist coordinates for suitable F) be a time function whose level sets are transversal to the future event and cosmological horizons. Let $\Sigma \subset t_*^{-1}(0)$ denote a spacelike hypersurface which extends a bit beyond the event and cosmological horizons. Suppose $\overline{g}$, K are solutions of the constraint equations (1.3) which are close (in the norm of $H^{21}(\Sigma; S^2T^*\Sigma)$) to the initial data at Σ of the metric g_{Λ,M_i,a_i}. Then on $\mathcal{M} = [0, \infty)_{t_*} \times \Sigma$ there exists a solution g of the initial value problem for* $\mathrm{Ric}(g) - \Lambda g = 0$ *which decays exponentially fast to a Kerr–de Sitter metric: there exist $M_f > 0$ and $a_f \in \mathbb{R}$, with (M_f, a_f) close to (M_i, a_i), and $\alpha > 0$ so that*

$$g = g_{\Lambda,M_f,a_f} + \tilde{g}, \quad \tilde{g} = \mathcal{O}(e^{-\alpha t_*}).$$

In particular, by the stable manifold theorem, the event and cosmological horizons of the perturbed spacetime $(\mathcal{M}, g)$ are exponentially decaying (as $t_* \to \infty$) perturbations of the horizons of g_{Λ,M_f,a_f}; in other words, $(\mathcal{M}, g)$ contains these two future affine complete horizons. For partial results on the stability of the cosmological (asymptotically de Sitter) part of Kerr–de Sitter spacetimes, see **[190, 191]**.

To complete the discussion of the proof of Theorem 15, we explain a few aspects of the (non-)linear analysis on asymptotically Kerr–de Sitter spaces. The nonlinear iteration scheme used in the proof of Theorem 15 involves the global solution, at each step, of a linear wave equation

$$L_{M,a,\tilde{g},\vartheta} h = [\text{nonlinear error term}]. \tag{2.32}$$

Here $L_{M,a,\tilde{g},\vartheta}$ is a wave operator (acting on symmetric 2-tensors) on the spacetime $\mathcal{M}$ equipped with a metric $g_{\Lambda,M,a} + \tilde{g}$ that settles down exponentially fast to a KdS metric.

Thus, the spectral methods which are effective for providing sharp asymptotics of stationary problems need to be supplemented by estimates *on the nonstationary spacetime* which are effective for proving the sharp regularity of linear waves. Roughly speaking, given a solution h of the linear wave equation (2.32) which, together with a large number of derivatives, obeys a weak exponential bound $h = \mathcal{O}(e^{Ct_*})$ for some fixed C (such estimates are discussed below), one can rewrite this equation as

$$L_0 h = -\tilde{L}h,$$

where $L_0 = L_{M,a,0,0}$ is the stationary part and $\tilde{L} = L_{M,a,\tilde{g},\vartheta} - L_{M,a,0,0}$ the (second order) remainder *with exponentially decaying* $\mathcal{O}(e^{-\alpha t_*})$ *coefficients*. Spectral methods for L_0 thus give precise asymptotics for h up to errors with an extra $e^{-\alpha t_*}$ amount of decay relative to the a priori information on h, i.e., $\tilde{L}h = \mathcal{O}(e^{(C-\alpha)t_*})$. Full asymptotics for h can then be obtained by iteration.

It thus remains to show (arbitrarily) high regularity of h in a space allowing for a fixed amount of exponential growth. Energy estimates give a simple exponential bound in H^1. Higher regularity of h (in the *same* exponentially weighted space in time) is then proved by microlocal means: regularity of the initial data is propagated using the Duistermaat–Hörmander theorem for finite times; uniform control as $t_* \to \infty$ requires the use of radial point estimates (on exponentially weighted function spaces) near the horizons [111], and simple (since we are allowing for exponential growth of solutions) estimates at the trapped set [104, 110]. We remark that the use of Nash–Moser iteration requires the proof of *tame* versions of all these microlocal estimates; these were first given in [112].

Theorem 15 was subsequently extended by Hintz to the setting of charged black holes:

Theorem 16 ([105]). *The family of Kerr–Newman–de Sitter black holes with subextremal charge and small angular momenta is nonlinearly asymptotically stable. That is, the spacetime metric and electromagnetic 2-form evolving from a small perturbation of the initial data of such a Kerr–Newman–de Sitter black hole settle down exponentially fast to the metric and electromagnetic 2-form of a nearby Kerr–Newman–de Sitter metric in a suitable gauge (generalized harmonic gauge for the metric, generalized Lorenz gauge for the electromagnetic field).*

Previously, Hintz–Vasy [112] had shown the solvability of quasilinear wave equations on slowly rotating Kerr–de Sitter spacetimes (by combining microlocal and spectral methods as sketched above) assuming the absence of modes in the closed upper half-plane, following earlier work on asymptotically de Sitter spacetimes [102, 111].

2.5.3. The case $\Lambda < 0$

As in the case of the maximally symmetric solutions in Section 2.1.3, the $\Lambda < 0$ case (with reflective boundary conditions) may turn out to be the most difficult and constitutes a major outstanding problem in the field. The slow logarithmic rate obtained for the toy problem (see Section 2.3) lead [120] to conjecture nonlinear instability. However, there could be subtle cancelations entering the nonlinear dynamics that allow for some version of orbital stability. Note that the nature of the slow decay (which disappears if only finitely many modes are taken into account) makes detecting an instability in numerical simulations difficult. Finding an appropriate nonlinear toy problem where some of the difficulties can be understood seems to be a first step to attack this problem.

3. SINGULARITIES

We discuss results concerning singularities occurring in the interior of black holes in Section 3.1. Recent progress on naked singularities is discussed in Section 3.2.

3.1. The interior of black holes

Whereas the exterior (or, indeed, suitable neighborhoods of the exterior) of subextremal Kerr black holes is conjectured to be stable, the situation is different for the black hole *interior*. Note in particular that Kerr black holes with nonzero angular momentum have a nonempty Cauchy horizon, whereas Schwarzschild black holes have an entirely different interior structure, namely they have a terminal spacelike singularity across which the metric cannot be extended even as a continuous Lorentzian metric [188]. Regarding thus the interior structure rotating Kerr black holes as a reference point, a heuristic due to Simpson–Penrose [195] suggests that the Kerr Cauchy horizon is unstable, in the sense that for generic perturbations of the initial data the spacetime metric becomes singular at the Cauchy horizon. This is the content of Penrose's *Strong Cosmic Censorship* conjecture. The basic idea is that linear waves falling into the black hole are more and more blue-shifted as one approaches the Cauchy horizon, which when upgraded to the nonlinear setting is suggestive of the formation of a singularity. This heuristic also suggests a direct relationship between decay of perturbations in the black hole exterior and the regularity of the metric near the Cauchy horizon.

The precise notion of singularity to be used depends on the context. One notion [44] asks for the nonexistence of an extension of the spacetime with square integrable Christoffel symbols since square integrability is sufficient to make sense of the Einstein equations in a weak sense; other often used notions are $\mathcal{C}^2$-inextendibility, as it relates directly to the blow-up of curvature invariants such as the Kretschmann scalar, or $\mathcal{C}^0$-inextendibility of the metric. The current state-of-the-art in the vacuum case is the following *regularity* theorem; its proof uses the double gauge (which is particularly convenient also for locating the Cauchy horizon):

Theorem 17 ([60]). *Assume quantitative decay rates*[10] *of the metric and second fundamental form, along a spacelike hypersurface Σ_0 just beyond the event horizon, to the data of a subex-*

10 These assumptions are compatible with the conjectured nonlinear stability of the Kerr family.

tremal Kerr metric with nonzero angular momentum. Then the future development of these data has a nontrivial Cauchy horizon across which the metric is continuously extendible.

Related regularity results for the linear scalar wave equation were proved by Franzen [85,86] and Hintz [103]. Reading Theorem 17 as a statement about the stability of the interior structure of Kerr black holes, one may consider the analogous problem for the stability of the Schwarzschild singularity (which necessarily requires working in a restricted symmetry class to disallow Kerr behavior). This was tackled by Alexakis–Fournodavlos [3] in polarized axial symmetry; see also [84] on the behavior of linear waves in the Schwarzschild interior.

For de Sitter black holes, waves decay in the exterior at an exponential rate, and correspondingly the regularity of metrics or linear scalar waves is expected to be higher at the Cauchy horizon. Quantitatively, linear waves with energy decaying like $\mathcal{O}(e^{-\alpha t_*})$ have almost $H^{1/2+\alpha/\kappa}$-regularity across the Cauchy horizon (and arbitrary regularity in the angular variables), where κ is the surface gravity of the Cauchy horizon [113] (see also [49]). This regularity can exceed H^1 for certain black hole parameters [34]; heuristically this corresponds to the expectation that the analogue of Theorem 17 in such settings yields spacetimes which, even upon perturbation, can be extended with square integrable Christoffel symbols. For rigorous results in this direction, see [50–52].

The first result on the existence of *singularities* was obtained for the linear scalar wave equation on Reissner–Nordström spacetimes with nonzero charge by Luk–Oh [150]; the key is the identification of a conserved quantity along null infinity, the nonvanishing of which allows for the propagation of suitable lower bounds into the black hole interior which imply blow-up of energy at the Cauchy horizon. The result by Luk–Sbierski [156] proves blow-up under the assumption of pointwise *lower* bounds for the linear wave along the event horizon of rotating Kerr black holes; these lower bounds were proved in [11,106], as discussed in Section 2.3.3.

Singularity formation at the Cauchy horizon for solutions of the Einstein equation is thus far only known in spherical symmetry for suitable matter models. Christodoulou [41] proved the $\mathcal{C}^0$-formulation of the Strong Cosmic Censorship conjecture for the Einstein–real scalar field system in spherical symmetry. In the presence of charge, Dafermos [54] with Rodnianski [61], on the other hand, proved that $\mathcal{C}^0$-regularity *does* hold for the Einstein–*Maxwell*–real scalar field system; this was complemented by the following result on the genericity of $\mathcal{C}^2$-singularities (improved to $\mathcal{C}^{0,1}$ in [189]):

Theorem 18 ([151,152]). *The $\mathcal{C}^2$ formulation of the Strong Cosmic Censorship conjecture for the Einstein–Maxwell–real scalar field system in spherical symmetry (with 2-ended asymptotically flat initial data on $\mathbb{R} \times \mathbb{S}^2$) is true.*

On charged Reissner–Nordström–AdS black hole spacetimes (thus $\Lambda < 0$), the behavior of linear waves near the Cauchy horizon was understood only recently in a series of works by Kehle who proved $\mathcal{C}^0$ bounds [135] and generic energy blow-up [134,136] depending on the validity of a diophantine condition on the quasinormal modes. Part of the difficulty here is the particularly slow (logarithmic) decay on the exterior.

3.2. Naked singularities

The singularities discussed in Section 3.1—be they spacelike or null—all share the feature of being "behind" an event horizon of a black hole exterior possessing a complete null infinity. Penrose's *Weak Cosmic Censorship* conjecture asserts that this is generically the case for solutions arising from asymptotically flat initial data: singularities always occur in the causal future of an event horizon and can thus not communicate with asymptotic observers at infinity. In [42, 43] Christodoulou showed that the word "generic" is indeed necessary. He constructed solutions to the spherically symmetric Einstein scalar field system containing a naked singularity, i.e., spacetimes whose Penrose diagram looks as in Figure 11. In particular, the cone $\mathcal{N}$ is future null geodesically incomplete and does not extend to $\mathcal{O}$. This can be seen by the quantity $\frac{2m}{r}$ being bounded uniformly from below by a positive constant along $\mathcal{N}$, where m denotes the Hawking mass and r the area radius function of the spherically symmetric spacetime. In particular, one cannot make sense of the Einstein equations in any reasonable sense (in particular, not in the class of bounded variation) on or to the future of $\mathcal{O}$.

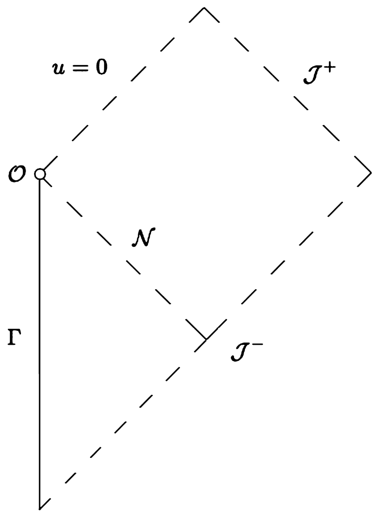

FIGURE 11
The naked singularity spacetimes of [42]. Here Γ denotes the center of the spherical symmetry. Null infinity $\mathcal{I}^+$ is future incomplete.

Christodoulou's construction relied on two fundamental ingredients. Let us denote a solution to the spherically symmetric Einstein scalar field system by $(g_{\mu\nu}, r, \phi)$. First, Christodoulou proved local well-posedness of the system in the (low regularity) class of BV solutions. Secondly, he introduced the notion of a k-self-similar solution of the system. This is a solution which admits a 1-parameter group of diffeomorphisms $(f_a)_{a\geq 0}$ such that $f_a^\star g = a^2 g$, $f_a^\star r = ar$ and $f_a^\star \phi = \phi - k \log a$. Imposing self-similarity and spherical symmetry reduces the Einstein equations to a two-dimensional autonomous dynamical system,

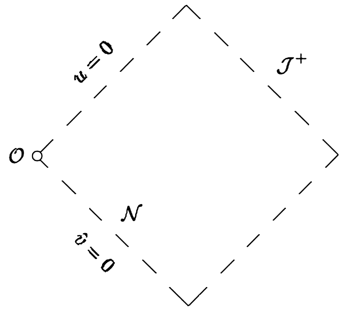

FIGURE 12

The naked singularity spacetimes of [183] arising from solving a characteristic initial value problem. Null infinity $\mathcal{J}^+$ is future incomplete.

whose dynamics Christodoulou analyzed. A suitable subset of its solutions could be interpreted as BV solutions (in fact they have higher regularity) and could be described by the above Penrose diagram. The key here is that the appearance of naked singularities fundamentally depends on k being *nonzero*.

In recent work, Rodnianski and Shlapentokh-Rothman transformed some of the above ideas to prove a result for the *vacuum equations without any symmetry assumptions*:

Theorem 19 ([183]). *There exists a large class of solutions to the vacuum Einstein equations containing naked singularities.*

The solutions of Theorem 19 are constructed directly by solving a characteristic initial value problem as discussed at the end of Section 1.3 leading to a Penrose diagram of the form shown in Figure 11.

The analogue of Christodoulou's well-posedness result for BV solutions in the proof of Theorem 19 is provided by the well-posedness theory that has been developed in recent years to construct low regularity solutions of the Einstein equations in a double null gauge, in particular the Luk–Rodnianski theory of impulsive gravitational waves [153,154][11] and the results of [182]. The idea is that one can construct solutions with very limited regularity in the null directions u and v but high regularity in the directions tangent to the double null spheres.

The analogue of Christodoulou's k-self-similar solutions can be described as follows. Assume momentarily that the solution has already been constructed in double null coordinates (note that the shift vector b has been put in the other null direction)

$$\begin{aligned} g &= -2\Omega^2(\mathrm{d}u \otimes \mathrm{d}v + \mathrm{d}v \otimes \mathrm{d}u) + \not{g}_{AB}(\mathrm{d}\theta^A - b^A \mathrm{d}u)(\mathrm{d}\theta^B - b^B \mathrm{d}u) \\ &= -2\Omega^2 v^{2\kappa}(1-2\kappa)^{-1}(\mathrm{d}u \otimes \mathrm{d}\hat{v} + \mathrm{d}\hat{v} \otimes \mathrm{d}u) + \not{g}_{AB}(\mathrm{d}\theta^A - b^A \mathrm{d}u)(\mathrm{d}\theta^B - b^B \mathrm{d}u), \end{aligned} \tag{3.1}$$

11 In this theory, the components α and $\underline{\alpha}$ are not even in L^2_u and L^2_v. They can, however, be removed from the system of double null equations by a clever renormalization of the system.

with the two sets of double null coordinates related by $\hat{v} = v^{1-2\kappa}$ for a small and positive κ.

We say that a solution is self-similar if the scaling vector field $S = u\partial_u + v\partial_v$ satisfies $\mathcal{L}_S g = 2g$. This directly translates into constraints on the behavior of the metric functions, for instance $\Omega(u, v, \theta^A) = \check{\Omega}(\frac{v}{u}, \theta^A)$, etc. The κ-self similarity now enters by imposing the manner in which the metric and its derivatives extend to the cone $\mathcal{N}$, i.e., the hypersurface $\hat{v} = 0$. A κ-self similar solution with $\kappa \neq 0$ is defined in a way that the metric and its derivatives extend regularly ($C^{1,\gamma}$) to $\mathcal{N}$ in the $(u, \hat{v}, \theta)$ coordinates. In the (u, v, θ) coordinates, however, quantities will then be singular with specific powers of $\frac{v}{u}$; in other words, (u, v, θ) coordinates are not regular on $\mathcal{N}$.

To view this more geometrically, note the difference of the generator of the null cone $\hat{v} = 0$ given by $e_3|_{\hat{v}=0} = \partial_u + \tilde{b}^A \partial_{\theta^A}$ and the restriction of the scaling field $S|_{\hat{v}=0} = u\partial_u$. If we can construct solutions with $\tilde{b} \neq 0$ along $\mathcal{N}$, then there will be a twisting of the generators by the self-similar vector field along $\mathcal{N}$. The point now is that if $\kappa = 0$, then the constraint equations along $\mathcal{N}$ necessitate $\tilde{b} = 0$ on $\mathcal{N}$. If $\kappa \neq 0$, then extra terms appear in the constraint equations which allow for nontrivial $\tilde{b}$; this is the main mechanism for the naked singularity formation (and for proving the analogue of $\frac{2m}{r}$ being bounded below along $\mathcal{N}$).

The proof itself has two main steps. The constraint equations need to be solved along the ingoing and outgoing light cones in a way that is consistent with the self-similarity of the solution and in a way that the low regularity well-posedness results mentioned earlier still apply. This requires (as expected from the nongenericity of naked singularities!) fine tuning of the "free data" (Section 1.3) and a detailed analysis of the regularity at the intersection of the two light cones. Once the data is constructed and the local well-posedness theorem applied, the proof proceeds in a large scale bootstrap argument to complete the picture shown in the Penrose diagram of Figure 12. This uses the familiar scheme of energy estimates for the curvature components and transport equations for the connection coefficients; however, many intricate renormalizations (subtracting the singular self-similar part of any dynamical quantity) and careful choices of $\frac{v}{u}$-weights in the estimates are required.

4. FURTHER TOPICS

We briefly discuss two more topics of continued or recent interest: the construction of multi-black-hole spacetimes, and inverse problems for nonlinear wave equations on Lorentzian manifolds.

4.1. Black hole gluing

All spacetimes discussed so far contain at most a single black hole. There exist explicit solutions of the Einstein–Maxwell equations without or with cosmological constant, called Majumdar–Papapetrou [158, 172] and Kastor–Traschen [132] spacetimes. They are, however, very rigid, being based on a special algebraic ansatz for the metric and electromagnetic field, in which the functions controlling the ansatz solve a linear Laplace equation and indeed are shifted and scaled versions of $1/|x|$. These spacetimes can be regarded as containing black holes each of which have charge equal to their mass. A construction due to Brill–Lindquist [30] produces a many-black-hole vacuum solution by similar rigid means.

The first flexible construction of many-black-hole spacetimes with well-controlled asymptotic structure glues any (finite) number of Kerr–de Sitter black holes into neighborhoods of points on the future conformal boundary of de Sitter space.

Theorem 20 ([107]). *Let* $\Lambda > 0$. *Fix points* $p_1, \ldots, p_N \in \mathbb{S}^3$, *masses* $M_1, \ldots, M_N$, *and angular momenta* $a_1, \ldots, a_N$; *assume that a certain balance condition holds. (When all* a_j *vanish, this balance condition reads* $\sum_{j=1}^N M_j p_j = 0$, *where one regards* $\mathbb{S}^3 \subset \mathbb{R}^4$ *as the unit sphere.) Then there exists a solution* g *of* $\mathrm{Ric}(g) - \Lambda g = 0$ *which near the point* p_j *on the future conformal boundary of de Sitter space is equal to* g_{Λ, M_j, a_j}, *and away from the points* p_j *converges to the de Sitter metric at an exponential rate.*

The gluing is accomplished via a backwards (or scattering) construction: a naively glued ansatz for the metric (which is an exact solution near the p_j) is corrected, *in the gluing region* (i.e., leaving neighborhoods of the p_j unaffected) [68], in Taylor series at the conformal boundary in a suitable generalised harmonic gauge, and the remaining error is solved away exactly by solving the gauge-fixed Einstein equation backwards from the conformal boundary. (See [56] for a loosely related scattering construction for asymptotically Kerr black holes.) The balance condition arises as an obstruction (cokernel) to the existence of a particular term in the Taylor expansion which needs to satisfy a linear divergence equation and yet have support away from the p_j.

Previous gluing constructions took place on the level of initial data sets, starting with Corvino's seminal work [47, 48] on localized gluing and followed by many variants and generalizations (including wormholes, localized gluing in angular sectors) [35, 46, 128, 129]. For recent gluing results for the characteristic initial value problem, see [16].

Chruściel–Mazzeo succeeded, using Friedrich's nonlinear stability result [87], in describing parts of the global structure of the spacetime evolving from the many-black-hole data of [46]; in particular, they show that the complement of the causal past of suitable observers at null infinity has several connected components, corresponding to several black hole regions. Analyzing the structure of compact subsets of these spacetimes is, however, entirely out of reach; the same is true for the spacetimes evolving from the initial data constructed numerically and used in numerical relativity for the study of black hole mergers [173].

The problem of constructing many-black-hole spacetimes with precise asymptotic control in the asymptotically flat setting (e.g., two Kerr black holes moving apart at a positive speed) is an interesting and challenging problem, (variants of) which may well be within reach in the near future.

4.2. Inverse problems

A rather different topic of investigation concerns the determination of a spacetime from measuring the propagation of waves inside the spacetime. This is typically phrased as the problem of reconstructing as large a spacetime region as possible from the Dirichlet-to-

Neumann map for boundary value problems for (nonlinear) wave equations on domains with timelike boundary, or from the source-to-solution map for forcing problems. For the linear wave equation on backgrounds *with time-independent metrics*, a complete solution of the first class of problems was obtained by Belishev–Kurylev [20] using a unique continuation result by Tataru [196].

A beautiful recent insight by Kurylev–Lassas–Uhlmann [143] is that nonlinearities can actually *simplify* the solution of the inverse problem, in particular in settings where the corresponding problem for the linear equation is not yet solved (e.g., for nonstationary metrics with nonanalytic time dependence).

The basic idea is that one can produce $\dim \mathcal{M} = 4$ small and mildly singular (distorted) plane wave solutions by imposing suitable Dirichlet boundary conditions or specifying suitable forcing terms. If these distorted plane waves interact nonlinearly at a spacetime point q, a new spherical wave is produced at q in the sense that a (very weak) singularity emanates from q; this singularity can be detected in the Neumann data or in some open set of the spacetime where one makes measurements. In this manner, the inverse problem is reduced to a geometric problem of reconstructing the Lorentzian structure (typically up to conformal diffeomorphisms) of a causal diamond $D \subset \mathcal{M}$ from the collection of the *light observation sets*—intersections of future light cones from points in q with the observation region. This geometric problem was solved in [143] for measurements in open subsets of $\mathcal{M}$, and in [109] for measurements on timelike boundaries under a convexity assumption.

There exists by now a large literature on similar inverse problems; here we only mention the results [142–144] on inverse problems concerned directly with the Einstein–scalar field and Einstein–Maxwell equations.

5. CONCLUSIONS AND OUTLOOK

The mathematical study of Einstein's theory of General Relativity is very natural: the main equation of the theory is "simple" despite being fundamental, i.e., not derived from a more general (classical) theory via any sort of approximation or averaging. And yet the structure of its solutions is fantastically rich, which thus provides a large arena for detailed investigations of various aspects of the theory.

It is a remarkable feature of general relativity that the simplest nontrivial vacuum spacetime—the Schwarzschild solution or its analogues in the presence of a nonzero cosmological constant—describes a *black hole*. (Moreover, even if the path of history was different, the study of (stationary) perturbations of the Schwarzschild solution could well have hinted at the existence of the Kerr family!) The study of perturbations of Schwarzschild or Kerr black holes in the context of the initial value problem can be regarded as a theoretical exploration of the question whether these solutions bear relevance as models for physical black holes. As discussed in Section 2, this line of investigation led to the discovery of fascinating geometric and analytic properties of Kerr spacetimes (such as the red-shift effect and superradiance, normally hyperbolic trapping, and mode stability), and inspired a vast amount of work, especially in the theory of partial differential equations, aimed at exploiting these properties (such as refined vector field methods, microlocal radial point and trapping estimates, flexible gauge-fixing methods). The confluence of a large variety of techniques from several areas of mathematics is the reason both for the recent success and for the excitement in the field. Given the progress discussed in Section 2, we anticipate a full resolution of the nonlinear stability problem for subextremal Kerr black holes in the near future. But even then will there be plenty of room for developments, e.g., coupling the Einstein equations with matter.

Analyzing the structure of singularities, whether cosmological, naked, or hidden behind event horizons of black holes, promises to continue being a fruitful area of research. In particular, controlling or constructing spacetimes with singularities requires the development of tools for the study of *large* data regimes (i.e., far from explicit model spacetimes), or calls for deep insights to find settings where large data regimes can still be regarded as perturbative in some sense.

The study of many-black-hole spacetimes has barely started. Motivated in particular by the recent experimental discoveries of black hole mergers, as well as by the advanced understanding of individual black holes, we anticipate this area of research to become prominent soon.

As the field advances, the technical demands will of course increase; however, we are confident that conceptual insights and the development of further elegant, yet powerful mathematical tools will act in a counterbalancing manner, thus keeping the field accessible and vibrant.

ACKNOWLEDGMENTS

The authors thank Gabriele Benomio, Mihalis Dafermos, Dejan Gajic, Yakov Shlapentokh-Rothman, and András Vasy for comments on the manuscript. G. Holzegel thanks Sakis Chatzikaleas for help with the pictures.

FUNDING

P. Hintz was partially supported by NSF Grant No. DMS-1955614 and a Sloan Research Fellowship. G. Holzegel acknowledges support by the Alexander von Humboldt Foundation in the framework of the Alexander von Humboldt Professorship endowed by the Federal Ministry of Education and Research and support by ERC Consolidator Grant 772249.

REFERENCES

[1] Oberwolfach report. 2021, preliminary version available at https://www.mfo.de/occasion/2135.

[2] S. Aksteiner and L. Andersson, Charges for linearized gravity. *Classical Quantum Gravity* **30** (2013), no. 15, 155016, 20 pp.

[3] S. Alexakis and G. Fournodavlos, Stable space-like singularity formation for axi-symmetric and polarized near-Schwarzschild black hole interiors. 2020, arXiv:2004.00692.

[4] M. T. Anderson, Existence and stability of even-dimensional asymptotically de Sitter spaces. *Ann. Henri Poincaré* **6** (2005), no. 5, 801–820.

[5] L. Andersson, T. Bäckdahl, P. Blue, and S. Ma, Stability for linearized gravity on the Kerr spacetime. 2019, arXiv:1903.03859.

[6] L. Andersson and P. Blue, Hidden symmetries and decay for the wave equation on the Kerr spacetime. *Ann. of Math.* **182** (2015), 787–853.

[7] Y. Angelopoulos, S. Aretakis, and D. Gajic, Horizon hair of extremal black holes and measurements at null infinity. *Phys. Rev. Lett.* **121** (2018), no. 13.

[8] Y. Angelopoulos, S. Aretakis, and D. Gajic, Late-time asymptotics for the wave equation on spherically symmetric, stationary spacetimes. *Adv. Math.* **323** (2018), 529–621.

[9] Y. Angelopoulos, S. Aretakis, and D. Gajic, Logarithmic corrections in the asymptotic expansion for the radiation field along null infinity. *J. Hyperbolic Differ. Equ.* **16** (2019), no. 01, 1–34.

[10] Y. Angelopoulos, S. Aretakis, and D. Gajic, Late-time asymptotics for the wave equation on extremal Reissner–Nordström backgrounds. *Adv. Math.* **375** (2020), 107363.

[11] Y. Angelopoulos, S. Aretakis, and D. Gajic, Late-time tails and mode coupling of linear waves on Kerr spacetimes. 2021, arXiv:2102.11884.

[12] Y. Angelopoulos, S. Aretakis, and D. Gajic, Price's law and precise late-time asymptotics for subextremal Reissner–Nordström black holes. 2021, arXiv:2102.11888.

[13] S. Aretakis, Stability and instability of extreme Reissner–Nordström black hole spacetimes for linear scalar perturbations I. *Comm. Math. Phys.* **307** (2011), no. 1, 17–63.

[14] S. Aretakis, Stability and instability of extreme Reissner–Nordström black hole spacetimes for linear scalar perturbations II. *Ann. Henri Poincaré* **12** (2011), no. 8, 1491–1538.

[15] S. Aretakis, Decay of axisymmetric solutions of the wave equation on extreme Kerr backgrounds. *J. Funct. Anal.* **263** (2012), no. 9, 2770–2831.

[16] S. Aretakis, S. Czimek, and I. Rodnianski, The characteristic gluing problem for the Einstein equations and applications. 2021, arXiv:2107.02441.

[17] V. Balasubramanian, A. Buchel, S. R. Green, L. Lehner, and S. L. Liebling, Holographic thermalization, stability of Anti-de Sitter space, and the Fermi–Pasta–Ulam paradox. *Phys. Rev. Lett.* **113** (2014), no. 7, 071601.

[18] D. Baskin, A. Vasy, and J. Wunsch, Asymptotics of radiation fields in asymptotically Minkowski space. *Amer. J. Math.* **137** (2015), no. 5, 1293–1364.

[19] D. Baskin, A. Vasy, and J. Wunsch, Asymptotics of scalar waves on long-range asymptotically Minkowski spaces. *Adv. Math.* **328** (2018), 160–216.

[20] M. Belishev and Y. Kurylev, To the reconstruction of a Riemannian manifold via its spectral data (BC–Method). *Comm. Partial Differential Equations* **17** (1992), no. 5–6, 767–804.

[21] A. N. Bernal and M. Sánchez, Smoothness of time functions and the metric splitting of globally hyperbolic spacetimes. *Comm. Math. Phys.* **257** (2005), no. 1, 43–50.

[22] N. Besset and D. Häfner, Existence of exponentially growing finite energy solutions for the charged Klein–Gordon equation on the de Sitter–Kerr–Newman metric. *J. Hyperbolic Differ. Equ.* **18** (2021), no. 02, 293–310.

[23] L. Bieri and N. Zipser, *Extensions of the stability theorem of the Minkowski space in general relativity*. AMS/IP Stud. Adv. Math. 45, American Mathematical Society, 2009.

[24] L. Bigorgne, D. Fajman, J. Joudioux, J. Smulevici, and M. Thaller, Asymptotic stability of Minkowski space-time with non-compactly supported massless Vlasov matter. *Arch. Ration. Mech. Anal.* **242** (2021), no. 1, 1–147.

[25] P. Bizoń and A. Rostworowski, Weakly turbulent instability of anti-de Sitter spacetime. *Phys. Rev. Lett.* **107** (2011), no. 3, 031102.

[26] P. Blue and A. Soffer, Semilinear wave equations on the Schwarzschild manifold. I. Local decay estimates. *Adv. Differential Equations* **8** (2003), no. 5, 595–614.

[27] P. Blue and A. Soffer, Errata for "Global existence and scattering for the nonlinear Schrodinger equation on Schwarzschild manifolds", "Semilinear wave equations on the Schwarzschild manifold I: Local Decay Estimates", and "The wave equation on the Schwarzschild metric II: Local Decay for the spin 2 Regge Wheeler equation". 2006, arXiv:gr-qc/0608073.

[28] J.-F. Bony and D. Häfner, Decay and non-decay of the local energy for the wave equation on the de Sitter–Schwarzschild metric. *Comm. Math. Phys.* **282** (2008), no. 3, 697–719.

[29] J.-F. Bony and D. Häfner, Low frequency resolvent estimates for long range perturbations of the Euclidean Laplacian. *Math. Res. Lett.* **17** (2010), no. 2, 303–308.

[30] D. R. Brill and R. W. Lindquist, Interaction energy in geometrostatics. *Phys. Rev.* **131** (1963), no. 1, 471.

[31] O. Brodbeck, S. Frittelli, P. Hübner, and O. A. Reula, Einstein's equations with asymptotically stable constraint propagation. *J. Math. Phys.* **40** (1999), no. 2, 909–923.

[32] G. A. Burnett, The high-frequency limit in general relativity. *J. Math. Phys.* **30** (1989), no. 1, 90–96.

[33] N. Burq, Décroissance de l'énergie locale de l'équation des ondes pour le problème extérieur et absence de résonance au voisinage du réel. *Acta Math.* **180** (1998), no. 1, 1–29.

[34] V. Cardoso, J. L. Costa, K. Destounis, P. Hintz, and A. Jansen, Quasinormal modes and strong cosmic censorship. *Phys. Rev. Lett.* **120** (2018), no. 3, 031103.

[35] A. Carlotto and R. Schoen, Localizing solutions of the Einstein constraint equations. *Invent. Math.* **205** (2016), no. 3, 559–615.

[36] B. Carter, Hamilton–Jacobi and Schrödinger separable solutions of Einstein's equations. *Comm. Math. Phys.* **10** (1968), no. 4, 280–310.

[37] M. Casals and P. Zimmerman, Perturbations of an extremal Kerr spacetime: analytic framework and late-time tails. *Phys. Rev. D* **100** (2019), no. 12.

[38] S. Chandrasekhar, *The mathematical theory of black holes*. Internat. Ser. Monogr. Phys. 69, The Clarendon Press, Oxford University Press, New York, 1992. Revised reprint of the 1983 original, Oxford Science Publications.

[39] Y. Choquet-Bruhat, Théorème d'existence pour certains systèmes d'équations aux dérivées partielles non linéaires. *Acta Math.* **88** (1952), no. 1, 141–225.

[40] Y. Choquet-Bruhat and R. Geroch, Global aspects of the Cauchy problem in general relativity. *Comm. Math. Phys.* **14** (1969), no. 4, 329–335.

[41] D. Christodoulou, The formation of black holes and singularities in spherically symmetric gravitational collapse. *Comm. Pure Appl. Math.* **44** (1991), no. 3, 339–373.

[42] D. Christodoulou, Examples of naked singularity formation in the gravitational collapse of a scalar field. *Ann. of Math.* (1994), 607–653.

[43] D. Christodoulou, The instability of naked singularities in the gravitational collapse of a scalar field. *Ann. of Math. (2)* **149** (1999), no. 1, 183–217.

[44] D. Christodoulou, *The formation of black holes in general relativity*. European Mathematical Society, 2009.

[45] D. Christodoulou and S. Klainerman, *The global nonlinear stability of the Minkowski space*. Princeton Math. Ser. 41, Princeton University Press, Princeton, NJ, 1993.

[46] P. T. Chruściel and E. Delay, On mapping properties of the general relativistic constraints operator in weighted function spaces, with applications. *Mém. Soc. Math. Fr. (N.S.)* **94** (2003), vi+103 pp.

[47] J. Corvino, Scalar curvature deformation and a gluing construction for the Einstein constraint equations. *Comm. Math. Phys.* **214** (2000), no. 1, 137–189.

[48] J. Corvino and R. M. Schoen, On the asymptotics for the vacuum Einstein constraint equations. *J. Differential Geom.* **73** (2006), no. 2, 185–217.

[49] J. L. Costa and A. T. Franzen, Bounded energy waves on the black hole interior of Reissner–Nordström–de Sitter. 2016, arXiv:1607.01018.

[50] J. L. Costa, P. M. Girão, J. Natário, and J. Drumond Silva, On the global uniqueness for the Einstein–Maxwell–scalar field system with a cosmological constant. II. Structure of the solutions and stability of the Cauchy horizon. *Comm. Math. Phys.* **339** (2015), no. 3, 903–947.

[51] J. L. Costa, P. M. Girão, J. Natário, and J. Drumond Silva, On the global uniqueness for the Einstein–Maxwell–scalar field system with a cosmological constant: I. Well posedness and breakdown criterion. *Classical Quantum Gravity* **32** (2015), no. 1, 015017, 33 pp. .

[52] J. L. Costa, P. M. Girão, J. Natário, and J. Drumond Silva, On the global uniqueness for the Einstein–Maxwell–scalar field system with a cosmological constant: III. Mass inflation and extendibility of the solutions. *Ann. PDE* **3** (2017), no. 1, 8.

[53] B. Craps, O. Evnin, and J. Vanhoof, Renormalization group, secular term resummation and AdS (in)stability. *J. High Energy Phys.* **10** (2014), 048.

[54] M. Dafermos, The interior of charged black holes and the problem of uniqueness in general relativity. *Comm. Pure Appl. Math.* **58** (2005), no. 4, 445–504.

[55] M. Dafermos and G. Holzegel, Dynamic instability of solitons in 4 + 1-dimensional gravity with negative cosmological constant (unpublished). 2006, https://www.dpmms.cam.ac.uk/~md384/ADSinstability.pdf.

[56] M. Dafermos, G. Holzegel, and I. Rodnianski, A scattering theory construction of dynamical vacuum black holes. 2013, arXiv:1306.5364.

[57] M. Dafermos, G. Holzegel, and I. Rodnianski, Boundedness and decay for the Teukolsky equation on Kerr spacetimes I: the case $|a| \ll M$. *Ann. PDE* **5** (2019), no. 1, 2.

[58] M. Dafermos, G. Holzegel, and I. Rodnianski, The linear stability of the Schwarzschild solution to gravitational perturbations. *Acta Math.* **222** (2019), 1–214.

[59] M. Dafermos, G. Holzegel, I. Rodnianski, and M. Taylor, The nonlinear stability of the Schwarzschild solution to gravitational perturbations. 2021, arXiv:2104.08222.

[60] M. Dafermos and J. Luk, The interior of dynamical vacuum black holes I: The C^0-stability of the Kerr Cauchy horizon. 2017, arXiv:1710.01722.

[61] M. Dafermos and I. Rodnianski, A proof of Price's law for the collapse of a self-gravitating scalar field. *Invent. Math.* **162** (2005), no. 2, 381–457.

[62] M. Dafermos and I. Rodnianski, The wave equation on Schwarzschild–de Sitter spacetimes. 2007, arXiv:0709.2766.

[63] M. Dafermos and I. Rodnianski, The red-shift effect and radiation decay on black hole spacetimes. *Comm. Pure Appl. Math.* **62** (2009), no. 7, 859–919.

[64] M. Dafermos and I. Rodnianski, Decay for solutions of the wave equation on Kerr exterior spacetimes I–II: the cases $|a| \ll M$ or axisymmetry. 2010, arXiv:1010.5132.

[65] M. Dafermos and I. Rodnianski, A new physical-space approach to decay for the wave equation with applications to black hole spacetimes. In *XVIth international congress on mathematical physics*, pp. 421–432, World Scientific, 2010.

[66] M. Dafermos, I. Rodnianski, and Y. Shlapentokh-Rothman, Decay for solutions of the wave equation on Kerr exterior spacetimes III: The full subextremal case $|a| < M$. *Ann. of Math. (2)* **183** (2016), no. 3, 787–913.

[67] M. Dafermos, I. Rodnianski, and Y. Shlapentokh-Rothman, A scattering theory for the wave equation on Kerr black hole exteriors. *Ann. Sci. Éc. Norm. Supér. (4)* **51** (2018), no. 2, 371–486.

[68] E. Delay, Smooth compactly supported solutions of some underdetermined elliptic PDE, with gluing applications. *Comm. Partial Differential Equations* **37** (2012), no. 10, 1689–1716.

[69] O. J. C. Dias, G. T. Horowitz, and J. E. Santos, Gravitational turbulent instability of Anti-de Sitter space. *Classical Quantum Gravity* **29** (2012), 194002.

[70] D. Dold, Unstable mode solutions to the Klein–Gordon equation in Kerr–anti-de Sitter spacetimes. *Comm. Math. Phys.* **350** (2017), no. 2, 639–697.

[71] R. Donninger, W. Schlag, and A. Soffer, A proof of Price's law on Schwarzschild black hole manifolds for all angular momenta. *Adv. Math.* **226** (2011), no. 1, 484–540.

[72] J. J. Duistermaat and L. Hörmander, Fourier integral operators. II. *Acta Math.* **128** (1972), no. 1, 183–269.

[73] S. Dyatlov, Exponential energy decay for Kerr–de Sitter black holes beyond event horizons. *Math. Res. Lett.* **18** (2011), no. 5, 1023–1035.

[74] S. Dyatlov, Quasi-normal modes and exponential energy decay for the Kerr–de Sitter black hole. *Comm. Math. Phys.* **306** (2011), no. 1, 119–163.

[75] S. Dyatlov, Asymptotic distribution of quasi-normal modes for Kerr–de Sitter black holes. *Ann. Henri Poincaré* **13** (2012), no. 5, 1101–1166.

[76] S. Dyatlov, Asymptotics of linear waves and resonances with applications to black holes. *Comm. Math. Phys.* **335** (2015), no. 3, 1445–1485.

[77] S. Dyatlov, Spectral gaps for normally hyperbolic trapping. *Ann. Inst. Fourier (Grenoble)* **66** (2016), no. 1, 55–82.

[78] S. Dyatlov and M. Zworski, *Mathematical theory of scattering resonances*. Grad. Stud. Math. 200, American Mathematical Society, 2019.

[79] D. Fajman, J. Joudioux, and J. Smulevici, The stability of the Minkowski space for the Einstein–Vlasov system. 2017, arXiv:1707.06141.

[80] F. Finster and J. Smoller, Decay of solutions of the Teukolsky equation for higher spin in the Schwarzschild geometry. *Adv. Theor. Math. Phys.* **13** (2009), no. 1, 71–110.

[81] F. Finster and J. Smoller, Linear stability of the non-extreme Kerr black hole. 2016, arXiv:1606.08005.

[82] G. Fournodavlos and J. Luk, Asymptotically Kasner-like singularities. 2020, arXiv:2003.13591.

[83] G. Fournodavlos, I. Rodnianski, and J. Speck, Stable Big Bang formation for Einstein's equations: the complete sub-critical regime. 2020, arXiv:2012.05888.

[84] G. Fournodavlos and J. Sbierski, Generic blow-up results for the wave equation in the interior of a Schwarzschild black hole. *Arch. Ration. Mech. Anal.* **235** (2020), no. 2, 927–971.

[85] A. T. Franzen, Boundedness of massless scalar waves on Reissner–Nordström interior backgrounds. *Comm. Math. Phys.* **343** (2016), no. 2, 601–650.

[86] A. T. Franzen, Boundedness of massless scalar waves on kerr interior backgrounds. *Ann. Henri Poincaré* **21** (2020), 1045–1111.

[87] H. Friedrich, On the existence of n-geodesically complete or future complete solutions of Einstein's field equations with smooth asymptotic structure. *Comm. Math. Phys.* **107** (1986), no. 4, 587–609.

[88] H. Friedrich, Einstein equations and conformal structure: existence of anti-de Sitter-type space-times. *J. Geom. Phys.* **17** (1995), no. 2, 125–184.

[89] J. Galkowski and M. Zworski, Analytic hypoellipticity of Keldysh operators. 2020, arXiv:2003.08106.

[90] O. Gannot, Quasinormal modes for Schwarzschild–AdS black holes: exponential convergence to the real axis. *Comm. Math. Phys.* **330** (2014), no. 2, 771–799.

[91] O. Gannot, Existence of quasinormal modes for Kerr–AdS black holes. *Ann. Henri Poincaré* **18** (2017), 2757–2788.

[92] E. Giorgi, The linear stability of Reissner–Nordström spacetime for small charge. *Ann. PDE* **6** (2020), no. 2, 1–145.

[93] C. R. Graham and J. M. Lee, Einstein metrics with prescribed conformal infinity on the ball. *Adv. Math.* **87** (1991), no. 2, 186–225.

[94] S. R. Green, A. Maillard, L. Lehner, and S. L. Liebling, Islands of stability and recurrence times in AdS. *Phys. Rev. D* **92** (2015), no. 8, 084001.

[95] C. Guillarmou and A. Hassell, Resolvent at low energy and Riesz transform for Schrödinger operators on asymptotically conic manifolds. I. *Math. Ann.* **341** (2008), no. 4, 859–896.

[96] C. Guillarmou and A. Hassell, Resolvent at low energy and Riesz transform for Schrödinger operators on asymptotically conic manifolds. II. *Ann. Inst. Fourier (Grenoble)* **59** (2009), no. 4, 1553–1610.

[97] C. Guillarmou, A. Hassell, and A. Sikora, Resolvent at low energy III: the spectral measure. *Trans. Amer. Math. Soc.* **365** (2013), no. 11, 6103–6148.

[98] C. Gundlach, G. Calabrese, I. Hinder, and J. M. Martín-García, Constraint damping in the Z4 formulation and harmonic gauge. *Classical Quantum Gravity* **22** (2005), no. 17, 3767.

[99] C. Gundlach, R. H. Price, and J. Pullin, Late-time behavior of stellar collapse and explosions. I. Linearized perturbations. *Phys. Rev. D* **49** (1994), no. 2, 883.

[100] D. Häfner, P. Hintz, and A. Vasy, Linear stability of slowly rotating Kerr black holes. *Invent. Math.* **223** (2021), 1227–1406.

[101] A. Hassell and A. Vasy, The resolvent for Laplace-type operators on asymptotically conic spaces. *Ann. Inst. Fourier* **51** (2001), 1299–1346.

[102] P. Hintz, Global analysis of quasilinear wave equations on asymptotically de Sitter spaces. *Ann. Inst. Fourier* **66** (2016), no. 4, 1285–1408.

[103] P. Hintz, Boundedness and decay of scalar waves at the Cauchy horizon of the Kerr spacetime. *Comment. Math. Helv.* **92** (2017), no. 4, 801–837.

[104] P. Hintz, Resonance expansions for tensor-valued waves on asymptotically Kerr–de Sitter spaces. *J. Spectr. Theory* **7** (2017), 519–557.

[105] P. Hintz, Non-linear stability of the Kerr–Newman–de Sitter family of charged black holes. *Ann. PDE* **4** (2018), no. 1, 11.

[106] P. Hintz, A sharp version of Price's law for wave decay on asymptotically flat spacetimes. 2020, arXiv:2004.01664.

[107] P. Hintz, Black hole gluing in de Sitter space. *Comm. Partial Differential Equations* **46** (2021), no. 7, 1280–1318.

[108] P. Hintz, Normally hyperbolic trapping on asymptotically stationary spacetimes. *Prob. Math. Phys.* **2** (2021), no. 1, 71–126.

[109] P. Hintz and G. Uhlmann, Reconstruction of Lorentzian manifolds from boundary light observation sets. *Int. Math. Res. Not.* (2018), rnx320.

[110] P. Hintz and A. Vasy, Non-trapping estimates near normally hyperbolic trapping. *Math. Res. Lett.* **21** (2014), no. 6, 1277–1304.

[111] P. Hintz and A. Vasy, Semilinear wave equations on asymptotically de Sitter, Kerr–de Sitter and Minkowski spacetimes. *Anal. PDE* **8** (2015), no. 8, 1807–1890.

[112] P. Hintz and A. Vasy, Global analysis of quasilinear wave equations on asymptotically Kerr–de Sitter spaces. *Int. Math. Res. Not.* **2016** (2016), no. 17, 5355–5426.

[113] P. Hintz and A. Vasy, Analysis of linear waves near the Cauchy horizon of cosmological black holes. *J. Math. Phys.* **58** (2017), no. 8, 081509.

[114] P. Hintz and A. Vasy, Asymptotics for the wave equation on differential forms on Kerr–de Sitter space. *J. Differential Geom.* **110** (2018), no. 2, 221–279.

[115] P. Hintz and A. Vasy, The global non-linear stability of the Kerr–de Sitter family of black holes. *Acta Math.* **220** (2018), 1–206.

[116] P. Hintz and A. Vasy, Stability of Minkowski space and polyhomogeneity of the metric. *Ann. PDE* **6** (2020), no. 2.

[117] P. Hintz and Y. Xie, Quasinormal modes of small Schwarzschild–de Sitter black holes. Preprint, 2020.

[118] M. W. Hirsch, C. C. Pugh, and M. Shub, *Invariant manifolds*. Lecture Notes in Math. 583, Springer, Berlin–New York, 1977.

[119] G. Holzegel, J. Luk, J. Smulevici, and C. Warnick, Asymptotic properties of linear field equations in anti-de Sitter space. *Comm. Math. Phys.* **374** (2020), no. 2, 1125–1178.

[120] G. Holzegel and J. Smulevici, Decay properties of Klein–Gordon fields on Kerr–AdS spacetimes. *Comm. Pure Appl. Math.* **66** (2013), no. 11, 1751–1802.

[121] G. Holzegel and J. Smulevici, Quasimodes and a lower bound on the uniform energy decay rate for Kerr–AdS spacetimes. *Anal. PDE* **7** (2014), no. 5, 1057–1090.

[122] G. T. Horowitz and J. E. Santos, Geons and the instability of Anti-de Sitter spacetime. *Surv. Differ. Geom.* **20** (2015), 321–335.

[123] C. Huneau and J. Luk, Trilinear compensated compactness and Burnett's conjecture in general relativity. 2019, arXiv:1907.10743.

[124] P.-K. Hung, The linear stability of the Schwarzschild spacetime in the harmonic gauge: odd part. 2018, arXiv:1803.03881.

[125] P.-K. Hung, The linear stability of the Schwarzschild spacetime in the harmonic gauge: even part. 2019, arXiv:1909.06733.

[126] P.-K. Hung, J. Keller, and M.-T. Wang, Linear stability of Schwarzschild spacetime: decay of metric coefficients. 2017, arXiv:1702.02843v3.

[127] A. Iantchenko, Quasi-normal modes for massless Dirac fields in Kerr–Newman–de Sitter black holes. 2015, arXiv:1511.09233.

[128] J. Isenberg, D. Maxwell, and D. Pollack, A gluing construction for non-vacuum solutions of the einstein-constraint equations. *Adv. Theor. Math. Phys.* **9** (2005), no. 1, 129–172.

[129] J. Isenberg, R. Mazzeo, and D. Pollack, Gluing and wormholes for the Einstein constraint equations. *Comm. Math. Phys.* **231** (2002), no. 3, 529–568.

[130] E. Y. Jaffe, Asymptotic description of the formation of black holes from short-pulse data. 2020, arXiv:2003.05985.

[131] T. Johnson, The linear stability of the Schwarzschild solution to gravitational perturbations in the generalised wave gauge. *Ann. PDE* **5** (2019), no. 2, 13.

[132] D. Kastor and J. Traschen, Cosmological multi-black-hole solutions. *Phys. Rev. D* **47** (1993), no. 12, 5370.

[133] B. S. Kay and R. M. Wald, Linear stability of Schwarzschild under perturbations which are non-vanishing on the bifurcation 2-sphere. *Classical Quantum Gravity* **4** (1987), no. 4, 893.

[134] C. Kehle, Diophantine approximation as Cosmic Censor for Kerr–AdS black holes. 2020, arXiv:2007.12614.

[135] C. Kehle, Uniform boundedness and continuity at the cauchy horizon for linear waves on Reissner–Nordström–AdS black holes. *Comm. Math. Phys.* **376** (2020), no. 1, 145–200.

[136] C. Kehle, Blowup of the local energy of linear waves at the Reissner–Nordström-AdS Cauchy horizon. *Classical Quantum Gravity* **38** (2021), 21.

[137] S. Klainerman and J. Szeftel, Constructions of GCM spheres in perturbations of Kerr. 2019, arXiv:1911.00697.

[138] S. Klainerman and J. Szeftel, Effective results on uniformization and intrinsic GCM spheres in perturbations of Kerr. 2019, arXiv:1912.12195.

[139] S. Klainerman and J. Szeftel, *Global nonlinear stability of Schwarzschild space-time under polarized perturbations: (AMS-210)*. Princeton University Press, 2021.

[140] S. Klainerman and J. Szeftel, Kerr stability for small angular momentum. 2021, arXiv:2104.11857.

[141] H. Kodama and A. Ishibashi, A master equation for gravitational perturbations of maximally symmetric black holes in higher dimensions. *Progr. Theoret. Phys.* **110** (2003), no. 4, 701–722.

[142] Y. Kurylev, M. Lassas, L. Oksanen, and G. Uhlmann, Inverse problem for Einstein-scalar field equations. 2014, arXiv:1406.4776.

[143] Y. Kurylev, M. Lassas, and G. Uhlmann, Inverse problems for Lorentzian manifolds and non-linear hyperbolic equations. 2014, arXiv:1405.3386.

[144] M. Lassas, G. Uhlmann, and Y. Wang, Determination of vacuum space-times from the Einstein–Maxwell equations. 2017, arXiv:1703.10704.

[145] H. Lindblad, On the asymptotic behavior of solutions to the Einstein vacuum equations in wave coordinates. *Comm. Math. Phys.* **353** (2017), no. 1, 135–184.

[146] H. Lindblad and I. Rodnianski, The global stability of Minkowski space-time in harmonic gauge. *Ann. of Math. (2)* **171** (2010), no. 3, 1401–1477.

[147] H. Lindblad and M. Taylor, Global stability of Minkowski space for the Einstein–Vlasov system in the harmonic gauge. 2017, arXiv:1707.06079.

[148] O. Lindblad Petersen and A. Vasy, Analyticity of quasinormal modes in the Kerr and Kerr–de Sitter spacetimes. 2021, arXiv:2104.04500.

[149] J. Luk, On the local existence for the characteristic initial value problem in general relativity. *Int. Math. Res. Not.* **20** (2012), 4625–4678.

[150] J. Luk and S.-J. Oh, Proof of linear instability of the Reissner–Nordström Cauchy horizon under scalar perturbations. *Duke Math. J.* **166** (2017), no. 3, 437–493.

[151] J. Luk and S.-J. Oh, Strong cosmic censorship in spherical symmetry for two-ended asymptotically flat initial data I. The interior of the black hole region. *Ann. of Math.* **190** (2019), no. 1, 1–111.

[152] J. Luk and S.-J. Oh, Strong cosmic censorship in spherical symmetry for two-ended asymptotically flat initial data II: the exterior of the black hole region. *Ann. PDE* **5** (2019), no. 1, 6.

[153] J. Luk and I. Rodnianski, Local propagation of impulsive gravitational waves. *Comm. Pure Appl. Math.* **68** (2015), no. 4, 511–624.

[154] J. Luk and I. Rodnianski, Nonlinear interaction of impulsive gravitational waves for the vacuum Einstein equations. *Cambridge J. Math.* **5** (2017), no. 4, 435–570.

[155] J. Luk and I. Rodnianski, High-frequency limits and null dust shell solutions in general relativity. 2020, arXiv:2009.08968.

[156] J. Luk and J. Sbierski, Instability results for the wave equation in the interior of Kerr black holes. *J. Funct. Anal.* **271** (2016), no. 7, 1948–1995.

[157] S. Ma, Uniform energy bound and Morawetz estimate for extreme components of spin fields in the exterior of a slowly rotating Kerr black hole II: linearized gravity. 2017, arXiv:1708.07385.

[158] S. D. Majumdar, A class of exact solutions of Einstein's field equations. *Phys. Rev.* **72** (1947), no. 5, 390.

[159] J.-A. Marck, Parallel-tetrad on null geodesics in Kerr–Newman space-time. *Phys. Lett. A* **97** (1983), no. 4, 140–142.

[160] R. R. Mazzeo and R. B. Melrose, Meromorphic extension of the resolvent on complete spaces with asymptotically constant negative curvature. *J. Funct. Anal.* **75** (1987), no. 2, 260–310.

[161] R. B. Melrose, *The Atiyah–Patodi–Singer index theorem*. Res. Notes Math. 4, A K Peters, Ltd., Wellesley, MA, 1993.

[162] R. B. Melrose, Spectral and scattering theory for the Laplacian on asymptotically Euclidian spaces. In *Spectral and scattering theory (Sanda, 1992)*, pp. 85–130, Lect. Notes Pure Appl. Math. 161, Dekker, New York, 1994.

[163] R. B. Melrose, A. Sá Barreto, and A. Vasy, Analytic continuation and semiclassical resolvent estimates on asymptotically hyperbolic spaces. *Comm. Partial Differential Equations* **39** (2014), no. 3, 452–511.

[164] R. B. Melrose, A. Sá Barreto, and A. Vasy, Asymptotics of solutions of the wave equation on de Sitter–Schwarzschild space. *Comm. Partial Differential Equations* **39** (2014), no. 3, 512–529.

[165] J. Metcalfe, J. Sterbenz, and D. Tataru, Local energy decay for scalar fields on time dependent non-trapping backgrounds. *Amer. J. Math.* **142** (2020), no. 3.

[166] V. Moncrief, Gravitational perturbations of spherically symmetric systems. I. The exterior problem. *Ann. Physics* **88** (1974), no. 2, 323–342.

[167] K. Morgan and J. Wunsch, Generalized Price's law on fractional-order asymptotically flat stationary spacetimes. 2021, arXiv:2105.02305.

[168] G. Moschidis, The r^p-weighted energy method of Dafermos and Rodnianski in general asymptotically flat spacetimes and applications. *Ann. PDE* **2** (2016), no. 1, 1–194.

[169] G. Moschidis, A proof of the instability of AdS for the Einstein–massless Vlasov system. 2018, arXiv:1812.04268.

[170] E. T. Newman, E. Couch, K. Chinnapared, A. Exton, A. Prakash, and R. Torrence, Metric of a rotating, charged mass. *J. Math. Phys.* **6** (1965), no. 6, 918–919.

[171] J. R. Oppenheimer and H. Snyder, On continued gravitational contraction. *Phys. Rev.* **56** (1939), no. 5, 455.

[172] A. Papapetrou, A static solution of the equations of the gravitational field for an arbitary charge-distribution. *Proc. R. Ir. Acad., A Math. Phys. Sci.* **51** (1945), 191–204.

[173] F. Pretorius, Evolution of binary black-hole spacetimes. *Phys. Rev. Lett.* **95** (2005), 121101.

[174] F. Pretorius and W. Israel, Quasi-spherical light cones of the Kerr geometry. *Classical Quantum Gravity* **15** (1998), no. 8, 2289.

[175] R. H. Price, Nonspherical perturbations of relativistic gravitational collapse. I. Scalar and gravitational perturbations. *Phys. Rev. D* **5** (1972), no. 10, 2419.

[176] R. H. Price and L. M. Burko, Late time tails from momentarily stationary, compact initial data in Schwarzschild spacetimes. *Phys. Rev. D* **70** (2004), no. 8, 084039.

[177] T. Regge and J. A. Wheeler, Stability of a Schwarzschild singularity. *Phys. Rev.* **108** (1957), 1063–1069.

[178] A. D. Rendall, Reduction of the characteristic initial value problem to the Cauchy problem and its applications to the Einstein equations. *Proc. R. Soc. Lond. Ser. A, Math. Phys. Sci.* **427** (1990), no. 1872, 221–239.

[179] H. Ringström, Future stability of the Einstein–non-linear scalar field system. *Invent. Math.* **173** (2008), no. 1, 123–208.

[180] H. Ringström, *The Cauchy problem in general relativity*. ESI Lect. Math. Phys. 6, European Mathematical Society, 2009.

[181] H. Ringström, On the geometry of silent and anisotropic big bang singularities. 2021, arXiv:2101.04955.

[182] I. Rodnianski and Y. Shlapentokh-Rothman, The asymptotically self-similar regime for the Einstein vacuum equations. *Geom. Funct. Anal.* **28** (2018), no. 3, 755–878.

[183] I. Rodnianski and Y. Shlapentokh-Rothman, Naked singularities for the Einstein vacuum equations: the exterior solution. 2019, arXiv:1912.08478.

[184] A. Rostworowski, Higher order perturbations of anti-de Sitter space and time-periodic solutions of vacuum Einstein equations. *Phys. Rev. D* **95** (2017), no. 12, 124043.

[185] X. Saint-Raymond, A simple Nash–Moser implicit function theorem. *Enseign. Math. (2)* **35** (1989), no. 3–4, 217–226.

[186] J. Sbierski, Characterisation of the energy of Gaussian beams on Lorentzian manifolds: with applications to black hole spacetimes. *Anal. PDE* **8** (2015), no. 6, 1379–1420.

[187] J. Sbierski, On the existence of a maximal Cauchy development for the Einstein equations: a dezornification. *Ann. Henri Poincaré* **17** (2016), no. 2, 301–329.

[188] J. Sbierski, The C_0-inextendibility of the Schwarzschild spacetime and the spacelike diameter in Lorentzian geometry. *J. Differential Geom.* **108** (2018), no. 2, 319–378.

[189] J. Sbierski, On holonomy singularities in general relativity and the $C^{0,1}_{\mathrm{loc}}$ inextendibility of spacetimes. 2020, arXiv:2007.12049.

[190] V. Schlue, Global results for linear waves on expanding Kerr and Schwarzschild de Sitter cosmologies. *Comm. Math. Phys.* **334** (2015), no. 2, 977–1023.

[191] V. Schlue, Decay of the Weyl curvature in expanding black hole cosmologies. 2016, arXiv:1610.04172.

[192] Y. Shlapentokh-Rothman, Exponentially growing finite energy solutions for the Klein–Gordon equation on sub-extremal Kerr spacetimes. *Comm. Math. Phys.* **329** (2014), no. 3, 859–891.

[193] Y. Shlapentokh-Rothman, Quantitative mode stability for the wave equation on the Kerr spacetime. *Ann. Henri Poincaré* **16** (2015), no. 1, 289–345.

[194] Y. Shlapentokh-Rothman and R. Teixeira da Costa, Boundedness and decay for the Teukolsky equation on Kerr in the full subextremal range $|a| < M$: frequency space analysis. 2020, arXiv:2007.07211.

[195] M. Simpson and R. Penrose, Internal instability in a Reissner–Nordström black hole. *Internat. J. Theoret. Phys.* **7** (1973), no. 3, 183–197.

[196] D. Tataru, Unique continuation for operators with partially analytic coefficients. *J. Math. Pures Appl.* **78** (1999), no. 5, 505–521.

[197] D. Tataru, Local decay of waves on asymptotically flat stationary space-times. *Amer. J. Math.* **135** (2013), no. 2, 361–401.

[198] D. Tataru and M. Tohaneanu, A local energy estimate on Kerr black hole backgrounds. *Int. Math. Res. Not.* **2011** (2011), no. 2, 248–292.

[199] M. Taylor, The global nonlinear stability of Minkowski space for the massless Einstein–Vlasov system. *Ann. PDE* **3** (2017), no. 1, 9.

[200] S. A. Teukolsky, Perturbations of a rotating black hole. I. Fundamental equations for gravitational, electromagnetic, and neutrino-field perturbations. *Astrophys. J.* **185** (1973), 635–648.

[201] A. Vasy, Microlocal analysis of asymptotically hyperbolic and Kerr–de Sitter spaces (with an appendix by Semyon Dyatlov). *Invent. Math.* **194** (2013), no. 2, 381–513.

[202] A. Vasy, Resolvent near zero energy on Riemannian scattering (asymptotically conic) spaces. 2018, arXiv:1808.06123.

[203] A. Vasy, Limiting absorption principle on Riemannian scattering (asymptotically conic) spaces, a Lagrangian approach. *Comm. Partial Differential Equations* (to appear).

[204] A. Vasy, Resolvent near zero energy on Riemannian scattering (asymptotically conic) spaces, a Lagrangian approach. *Comm. Partial Differential Equations* (to appear).

[205] A. Vasy and M. Zworski, Semiclassical estimates in asymptotically Euclidean scattering. *Comm. Math. Phys.* **212** (2000), no. 1, 205–217.

[206] C. V. Vishveshwara, Stability of the Schwarzschild metric. *Phys. Rev. D* **1** (1970), 2870–2879.

[207] R. M. Wald, Note on the stability of the Schwarzschild metric. *J. Math. Phys.* **20** (1979), no. 6, 1056–1058.

[208] C. M. Warnick, On quasinormal modes of asymptotically anti-de Sitter black holes. *Comm. Math. Phys.* **333** (2015), no. 2, 959–1035.

[209] B. F. Whiting, Mode stability of the Kerr black hole. *J. Math. Phys.* **30** (1989), no. 6, 1301–1305.

[210] J. Wunsch and M. Zworski, Resolvent estimates for normally hyperbolic trapped sets. *Ann. Henri Poincaré* **12** (2011), no. 7, 1349–1385.

[211] F. J. Zerilli, Effective potential for even-parity Regge–Wheeler gravitational perturbation equations. *Phys. Rev. Lett.* **24** (1970), 737–738.

PETER HINTZ

ETH Zürich, Departement Mathematik, Rämistrasse 101, 8092 Zürich, Switzerland, peter.hintz@math.ethz.edu

GUSTAV HOLZEGEL

Universität Münster, Mathematisches Institut, Einsteinstrasse 62, 48149 Münster, Germany, gholzege@uni-muenster.de